ANDRE SOUTHERNMAN TEIXEIRA IRSIGLER

TRANSCRIPTIONAL PROFILING REVEALS OVERLAP BETWEEN ER- AND OSMOTIC-STRESS RESPONSES IN SOYBEAN

Tese apresentada à Universidade Federal de Viçosa, como parte das exigências do Programa de Pós-Graduação em Genética e Melhoramento, para obtenção do título de *Doctor Scientiae*.

VIÇOSA
MINAS GERAIS - BRASIL
2006

ANDRE SOUTHERNMAN TEIXEIRA IRSIGLER

TRANSCRIPTIONAL PROFILING REVEALS OVERLAP BETWEEN ER- AND OSMOTIC-STRESS RESPONSES IN SOYBEAN

Tese apresentada à Universidade Federal de Viçosa, como parte das exigências do Programa de Pós-Graduação em Genética e Melhoramento, para obtenção do título de *Doctor Scientiae*.

APROVADA: 18 de dezembro de 2006.

_____
Prof. Sérgio H. Brommonschenkel
(Co-orientador)

_____
Profª. Juliana Lopes Rangel Fietto

_____
Prof. Gilberto Sachetto Martins

_____
Prof. Luciano Gomes Fietto
(Co-orientador)

_____
Profª. Elizabeth Pacheco B. Fontes
(Orientadora)

To my precious son, Luca

AGRADECIMENTOS

Gostaria de agradecer primeiramente minha esposa Danielle, em consideração a todo seu suporte, compreensão e carinho.

Agradeço também:

Minha orientadora Dra. Elizabeth Fontes, que me encorajou, e possibilitou este trabalho de ser realizado, com suas sugestões, estrutura de laboratório, e seus conhecimentos técnicos e científicos, e todos meus amigos membros de seu laboratório pelo ótimo ambiente de trabalho;

Dra. Rebecca Boston, por mais que o suporte em seu laboratório, mas por ser uma grande orientadora e exemplo de boa pesquisadora, e Dr. Jeff Gillikin e outros do laboratório, por toda a assistência e amizade.

Dr. Ralph Dewey, pela biblioteca de cDNA de soja e recursos de "microarrays", e amigos Dr. Karthik Aghoram, Dr. Steven Bowen e Ping Zhang;

o grupo do Laboratório de Pesquisas Genômicas (GRL) / NCSU, pela estrutura fornecida, que possibilitou a produção e análise dos "microarrays";

Dra. Judith Thomas e funcionários do Phytotron-NCSU, pelo espaço nas câmaras de crescimento de plantas e assistência no crescimento de plantas de soja;

os técnicos nas casas de vegetação na UFV, pelo espeço e recursos para realizar os experimentos com plants de soja;

Dr. Sérgio Brommonschenkel, e membros de seu laboratório, em especial Dra. Elene Yamazaki, pela estrutura no laboratório e ajuda nas análises de RT-PCR em tempo real;

toda minha família, em especial minha mãe e avó Maria Célia e Célia, e pai e avô Rodolfo e Mozart (que sei que ambos estão no céu iluminando meus caminhos), meu irmão David, e meus tios e tias, primos, meu sobrinho, e todos meus amigos;

as agências CAPES e CNPq, pelo suporte financeiro;

a Universidade Federal de Viçosa e North Carolina State University, por toda a estrutura acadêmica;

e todos aqueles que direta ou indiretamente deram suporte a este trabalho.

BIOGRAFIA

Nascido em São Paulo em 1978, André Southernman Teixeira Irsigler, o segundo filho de Maria Célia Couto Teixeira e Ernesto Rodolfo Irsigler, viveu a maior parte de sua infância na cidade de Juiz de Fora, Minas Gerais. Foi para a cidade de Viçosa, Minas Gerais, para estudar Biologia, e no ano 2000 obteve o grau de bacharel em Ciências Biológicas pela Universidade Federal de Viçosa. Como estudante de graduação, André foi membro do Programa Especial de Treinamento (PET/CAPES), sob a supervisão do Prof. Dr. Lúcio Campos, e se envolveu também no ensino como tutor em cursos de genética e biologia celular, e também em pesquisa em genética de abelhas, com o Dr. Lúcio Campos. Em 2002 recebeu o título de mestre, trabalhando na mesma área, no programa de Genética e Melhoramento da UFV. Iniciou seu doutorado no mesmo programa em 2002, com a Dra. Elizabeth Fontes, trabalhando com biologia molecular de soja. Em 2003 foi para a North Carolina State University realizar parte de suas pesquisas com a Dra. Rebecca Boston, e em 2006 se tornou associado ao Departamento de Biologia da Florida State University como Especialista em Pesquisa no Molecular Core Facility.

SUMÁRIO

RESUMO

IRSIGLER, André Southernman Teixeira, D.Sc., Universidade Federal de Viçosa, dezembro de 2006. **Perfilização transcricional revela sobreposição entre as respostas induzidas por estresses osmótico e do retículo endoplasmático em soja.** Orientadora: Elizabeth Pacheco Batista Fontes. Co-orientadores: Sérgio Hermínio Brommonschenkel e Luciano Gomes Fietto.

Embora a via de resposta a estresse do retículo endoplasmático (RE) seja potencialmente capaz de acomodar vias adaptativas, a sua integração com outras vias de sinalização, induzidas por condições adversas do meio ambiente, não tem sido analisada em plantas. Neste estudo, foi conduzida uma análise do perfil da expressão gênica global em folhas de soja expostas ao tratamento com polietileno glicol ou a indutores da resposta a proteínas mal-dobradas (UPR), a fim de identificar redes de integração entre respostas adaptativas induzidas por estresses osmótico e do RE. Os resultados revelaram os ramos principais da resposta ao estresse do RE, que incluem o aumento no dobramento e degradação de proteínas no RE, assim como mudanças específicas reguladas por desequilíbrio osmótico e ligadas a respostas celulares induzidas por desidratação. No entanto, uma pequena porção (5.5%) do total de genes regulados positivamente representou uma resposta comum que parece integrar as duas vias de sinalização. Estes genes co-regulados foram considerados alvos “downstream” dessa via de integração, baseado na cinética de indução e na resposta sinergística à combinação de tratamentos indutores dos estresses osmótico e do RE. Os genes nesta via de integração que exibiram intenso sinergismo de resposta codificam proteínas com diferentes funções. Duas delas contêm um domínio de desenvolvimento e morte celular (DCD) planta-específico, enquanto que

uma outra tem homologia a proteínas com um domínio associado a ubiquitina (UBA). Uma proteína contendo o domínio NAC exibiu uma cinética de indução precoce e robusta, consistente com sua função como transfator. Esta via integrada divergiu daqueles ramos da UPR já caracterizados e que são específicos de estresses no RE, uma vez que os genes alvos foram inversamente regulados por estresse osmótico. Coletivamente, estes resultados descrevem um novo ramo da resposta ao estresse do RE que integra o sinal osmótico para potenciar transcrição de genes alvos comuns.

ABSTRACT

IRSIGLER, André Southernman Teixeira, D.Sc., Universidade Federal de Viçosa, December of 2006. **Transcriptional profiling reveals overlap between ER- and osmotic-stress responses in soybean.** Adviser: Elizabeth Pacheco Batista Fontes. Co-Advisers: Sérgio Hermínio Brommonschenkel and Luciano Gomes Fietto.

Despite the potential of the endoplasmic reticulum (ER) stress response to accommodate adaptive pathways, its integration with other environmental-induced responses is poorly understood in plants. Here, we performed global expression profiling on soybean leaves exposed to polyethylene glycol treatment or to unfolded protein response (UPR) inducers to identify integrated networks between osmotic and ER stress-induced adaptive responses. The results unmasked the major branches of the ER-stress response, which includes enhancing protein folding and degradation in the ER, as well as specific osmotically regulated changes linked to cellular responses induced by dehydration. However, a small proportion (5.5%) of total up-regulated genes represented a shared response that seemed to integrate the two signaling pathways. These co-regulated genes were considered downstream targets based on similar induction kinetics and a synergistic response to the combination of osmotic- and ER-stress-inducing treatments. Genes in this integrated pathway with the strongest synergistic induction encoded proteins with diverse roles. Two of them contained a plant-specific development and cell death (DCD) domain while another had homology to proteins with an ubiquitin-associated (UBA) domain. A NAC domain-containing protein exhibited robust early kinetics of induction consistent with a role as a transfactor. This integrated pathway diverged

further from characterized ER-specific branches of UPR as downstream targets were inversely regulated by osmotic stress. Collectively, our results describe a novel branch of the ER stress response that integrates the osmotic signal to potentiate transcription of shared target genes.

Introduction

Environmental stress conditions, such as water deficit, extremes of temperature and high-salinity, are major constraints for plant growth, crop productivity, and distribution. Different approaches to increase stress tolerance in plants have been undertaken, such as manipulating and reprogramming the expression of endogenous stress-related genes (for review see Mahajan and Tuteja, 2005). In general, strategies targeting expression of transcription factors and other regulatory genes have been effective by the consequent up-regulation of many downstream genes (Jaglo-Ottosen et al., 1998; Kasuga et al., 1999; Hsieh et al., 2002; Hu et al., 2006). However, enhanced stress tolerance has also been achieved by changing the expression of a single downstream gene (Bartels, 2001; Zhu, 2001). In this case, effective targets for engineering stress tolerance include genes involved in mechanisms that prevent intracellular stress build up, like the Na+/H+-antiporter gene (Apse et al., 1999), as well as those directly involved in cellular protection and repair, such as the antioxidant system and molecular chaperone genes (Gupta et al., 1993; Wehmeyer and Vierling, 2000; Badawi et al., 2004; Rodrigues et al., 2006). The endoplasmic reticulum (ER) molecular chaperone BiP (Binding Protein), which provides cellular protection against ER stress in suspension cells and during seed germination, enhances tolerance to water dehydration when ectopically expressed in the model system tobacco (Alvim et al., 2001). Although the underlying mechanism for BiP-mediated increases in water-stress tolerance is not completely understood, the current knowledge of BiP function accommodates the argument that it may act in both mechanisms. In the first

case, BiP would interact with downstream targets during water stress, in the second, it would activate transmembrane kinases that signal the ER stress (Bertolotti et al., 2000; Okamura et al., 2000; Kimata et al., 2003; Kimata et al., 2004).

As an ER-resident molecular chaperone, BiP has a major function to enable folding of newly synthesized secretory proteins by preventing misfolding or aggregation of folding intermediates (Gething, 1999; Kleizen and Braakman, 2004; Ma and Hendershot, 2004). In addition, BiP is involved in several other ER-associated cellular processes, such as protein co-translational translocation (Sanders et al., 1992; Hamman et al., 1998), modulation of calcium storage (Lievremont et al., 1997), ER-associated protein degradation (ERAD; Nishikawa et al., 2001; Molinari et al., 2002) and signaling ER stress by sensing alterations in the ER environment (Bertolotti et al., 2000; Shen et al., 2002). Any stress conditions that disrupt ER homeostasis and promote accumulation of unfolded proteins in the organelle trigger a cytoprotective signaling cascade that has been studied in detail in yeast and mammalian cells, and designated the unfolded protein response (UPR).

In yeast, ER stress is sensed by the luminal domain of the ER transmembrane protein kinase Ire1p, which, upon dimerization of the cytosolic domain and subsequent activation of its kinase and endonuclease domains, activates downstream events. The hallmark of this ER-stress response is the coordinated up-regulation of ER molecular chaperones leading to an increase in the ER protein processing capacity to prevent protein aggregation (for review see Ma and Hendershot, 2004). In mammals,

the UPR is transduced by three distinct classes of ER transmembrane proteins: PERK, ATF6 and Ire1p homologues (Rao and Bredesen, 2004). Upon activation, these proteins act in concert to trigger a transient attenuation of protein synthesis, degradation of misfolded proteins and up-regulation of ER folding functions.

The mammalian Ire1p homologues, designated Ireα and Ireβ, are structurally organized into a luminal-stress sensing domain, a transmembrane segment and cytosolic kinase/endonuclease domains (Wang et al., 1998). The mammalian PERK is an eIF2-α kinase which inhibits protein translation in the early phase of the ER-stress response to maintain a proper balance between protein synthesis rate and ER processing capacity (Harding et al., 2000). ATF6 is a transcription factor that under normal conditions is anchored to the ER membrane, with a C-terminal ER-stress sensing domain oriented to the ER lumen (Haze et al., 1999). In response to ER stress, ATF6 is translocated to the Golgi, where it is specifically cleaved by S1P and S2P proteases to relieve its N-terminal transcription factor domain (Ye et al., 2000). The cleaved ATF6 domain is targeted to the nucleus where it drives the coordinated up-regulation of a set of genes encoding ER chaperones and folding enzymes. The ER molecular chaperone BiP directly regulates the UPR by controlling the activation status of the three classes of transducers (Bertolotti et al., 2000).

In plants, two Ire1p homologues have also been identified, but functional information is lacking and downstream components are yet to be identified (Koizumi et al., 2001). Recently, an ER-stress induced leucine zipper (bZIP) transcription factor gene from Arabidopsis, designated

AtbZIP60, has been shown to activate BiP and calnexin promoters through ER stress response element-like sequences (Iwata and Koizumi, 2005). AtbZIP60 is though to be anchored to the ER membrane under normal conditions but is released from the membrane upon sensing the ER stress by an unknown mechanism. The bZIP domain is translocated to the nucleus where activates the expression of molecular chaperones and its own expression. While the proposed initial trigger of AtbZIP60 activation by induced-conformational change resembles the mammalian ATF6 mechanism, its autoregulation is similar to that of XBP1 in mammalian cells.

Although little is known about the components of ER-stress signaling in plants, comprehensive genome-wide evaluations of the ER-stress-induced changes in gene expression have provided evidence that the major branches of the mammalian UPR are conserved in plants as well (Martinez and Chrispeels, 2003; Kamauchi et al., 2005). Likewise, genome-wide analyses and expression profiling studies in different plant species have revealed specific responses to wounding, drought, osmotic, cold and salt stresses, as well as the cross-talk between their signaling cascades (Kreps et al., 2002; Seki et al., 2002; Denekamp and Smeekens, 2003). Given the potential of BiP to regulate the UPR and the capacity of the BiP overexpressing plants to maintain leaf turgor under water deficit conditions (Bertolotti et al., 2000; Alvim et al., 2001), we reasoned that a genomic scale profile of the shared responses of ER and osmotic stresses would provide insights into the mechanism of BiP-mediated increases in osmotic balance under stress conditions. In addition to identifying ER-stress and osmotic-stress-specific responses in soybean (Glycine max), our global expression-profiling

analyses provided a list of candidate regulatory components, which may integrate the osmotic-stress and ER-stress signaling pathways in plants.

Literature Review

The endoplasmic reticulum (ER) and protein folding

The ER is a membranous cellular compartment, is the first destination for all the secretory proteins, and is responsible for the synthesis, modification and delivery of proteins to their proper sites within the secretory pathway. Proteins are directed to the ER through a hydrophobic signal sequence and traverse, either co- or post-translationally, the ER membrane through the Sec61p complex (Pilon et al., 1998). In the ER, nascent proteins find an optimal environment for folding into their native conformation, and undergo a series of post-translational modifications, including glycosylation (Hubbard and Ivatt, 1981; Kornfeld and Kornfeld, 1985) and formation of intra- and intermolecular disulfide bonds (Fewell et al., 2001).

The folding machinery in the ER consists of foldases, molecular chaperones, and lectins. Foldases catalyze steps in the protein folding. Example of foldases are protein disulfide isomerases (PDI), members of the superfamily of thioredoxin-domain-containing proteins, which catalyze the formation of disulfide bonds and play an important role in protein folding (Wilkinson and Gilbert, 2004; Houston et al., 2005). Molecular chaperones facilitate protein folding by protecting unfolded proteins from undesired interactions, keeping proteins in a folding-competent state. A major and well-characterized ER molecular chaperone is HSP70/BiP (Binding Protein) that, beside function in protein folding, has important roles in protein translocation and response to stress (Haas and Wabl, 1983; Dorner et al., 1992; Hamman

et al., 1998; Ellgaard et al., 1999). Lectins such as calnexin, calreticulin and ER degradation-enhancing α-mannosidase-like proteins (EDEM) interact with glycoproteins, assisting folding and quality control (Ellgaard and Helenius, 2003; Molinari et al., 2003; Oda et al., 2003).

The ER function and folding of proteins have been related to the production of reactive oxygen species (ROS), and consequent oxidative stress. During protein disulfide bond formation, PDI is reduced and then recycled by the FAD-dependent oxidases Ero1p and Erv2p (Frand and Kaiser, 1998; Pollard et al., 1998; Gerber et al., 2001). The final electron acceptor of Ero1p and Erv2p is O_2 (Tu et al., 2000; Sevier et al., 2001; Tu and Weissman, 2002), if uncoupled from other possible physiological electron acceptors, so far not yet identified. Although the cellular mechanisms preventing oxidative stress generated by disulfide bond formation remains unclear, the glutathione system represents a major redox buffer in the cell, and is an important component regulating the oxidative level of the ER (Tu and Weissman, 2004).

The unfolded protein response (UPR)

The accumulation of unfolded proteins in the ER is a major cause of ER stress, and can be a result of the high influx of nascent unfolded polypeptides in the ER, exceeding the ER folding capacity, or when there is an impediment for proper protein folding, such as prevention of post-translational modifications, unbalance of calcium in the ER, and errors in the primary structure of proteins. Such perturbations can affect ER function and

trigger the unfolded protein response (UPR). The UPR is coordinated pathways of signal transduction that normalize the ER function by increasing the protein folding capacity and decreasing the protein folding demand. To increase the folding capacity in the ER, the synthesis of ER-resident molecular chaperones and foldases is increased (Kozutsumi et al., 1988). The folding demand decreases by (1) downregulation of transcription and translation of genes encoding secretory proteins (Harding et al., 1999), (2) degradation of a specific subset of mRNAs (Hollien and Weissman, 2006), and (3) greater clearance of unfolded or misfolded proteins through ER-associated degradation (ERAD) (Travers et al., 2000).

Three main ER-transmembrane proteins, IRE1, ATF6 and PERK, are known to be signal transducers in the ER-stress response, and regulate a broad range of genes. IRE1 has a kinase and a endoribonuclease domain (Cox et al., 1993; Mori et al., 1993), and when activated promotes a nonconventional splicing and maturation of the mRNA that encodes the b-ZIP transcription factor Hac1p from yeast (Cox and Walter, 1996), homolog to the mammalian XBP-1 (Calfon et al., 2002). This transcription factor regulates expression of molecular chaperones, genes related to ERAD, and a range of secretory proteins. In mammalian cells the transcription factor ATF6, an ER-transmembrane protein that, under ER-stress, migrates to the Golgi and is activated by proteases to regulate a set of genes (Haze et al., 1999; Chen et al., 2002). PERK, another ER-transmembrane protein kinase, when activated by ER-stress, downregulates translation of proteins by phosphorylation of translation initiation factor two on its alpha subunit (eIF2α; (Harding et al., 2000).

The level and status of molecular chaperones possibly are major factors for sensing ER stress. Interactions between BiP and IRE1 or PERK have been demonstrated (Liu et al., 2002). BiP can be found in monomeric or oligomeric state. As an oligomer, BiP is modified by phosphorylation in its peptide-binding domain and ADP ribosylation (Gething, 1999). Only the monomer form can bind unfolded proteins (Gething, 1999) and ATP regulates the affinity of BiP to the substrate. The regulation of BiP and its property of recognizing and binding folding proteins, and interaction with UPR-related ER-membrane proteins suggest a possible mechanism for sensing ER-stress.

Protective role of molecular chaperones

Plants can be exposed to a diversity of environmental conditions that disrupt normal cellular function, eliciting a stress response that alters the plant physiology by regulating transcription of a large number of genes. Heat shock proteins (HSPs) function as molecular chaperones, maintaining proteins in a folding-competent state, and minimizing aggregation and accumulation of non-native proteins. Many genes encoding HSPs respond to a wide variety of stresses (Feder and Hofmann, 1999), possibly representing elements involved in stress tolerance mechanisms. Consistently, small HSPs have been associated with plant desiccation tolerance (Almoguera and Jordano, 1992; Wehmeyer and Vierling, 2000). Moreover, the overexpression of an ABA- inducible HSP70 in transgenic tobacco plants has been correlated to drought-stress tolerance (Cho and Hong, 2006).

In the ER, the binding protein HSP70/BiP is one of the major molecular chaperones induced by ER stress, participating in the translocation and folding of proteins, and sensing and signaling the ER stress (Haas and Wabl, 1983; Dorner et al., 1992; Hamman et al., 1998; Ellgaard et al., 1999). Previous studies suggest the involvement of BiP in stress tolerance. Overexpression of BiP in mammalian cultured cells (Dorner et al., 1992; Morris et al., 1997) and tobacco protoplasts (Leborgne-Castel et al., 1999) alleviates or prevents the induction of UPR-induced genes. In tobacco plants, overexpression of BiP leads to tolerance to water deficit, preventing decreases in photosynthesis and water content in plants submitted to water deprivation (Alvim et al., 2001). Although the mechanism of BiP-mediated water stress tolerance is not well understood, the observation that the anti-oxidative response normally caused by water-stress is not activated in drought-treated transgenic plants overexpressing BiP (Alvim et al., 2001), suggests that overexpression of BiP in plants may prevent endogenous oxidative stress.

Material and Methods

Plant growth and stress treatments

For the microarray experiments, soybean (*Glycine max*) seeds (cultivar Dare) were germinated in soil (MetroMix-360, Scotts, Marysville, OH) in a growth chamber with a day/night cycle of 9/15 h at 26°C/22°C. The aerial portions of three-week-old plants were excised below the cotyledons and directly placed into 15 ml of 10% (w/v) polyethylene glycol (PEG; MW 8000, Sigma, St. Louis, MO), 10 µg/ml tunicamycin (Sigma) or 50 mM L-azetidine-2-carboxylic acid (AZC, Sigma) solutions. The first trifoliate leaves were harvested after 16 h of PEG or AZC treatment (water control) and after 24 h of tunicamycin treatment (DMSO control, Sigma), then immediately frozen in liquid N_2 and stored at -80°C until use. In all experiments two independent biological replicates were used.

For the real-time RT-PCR experiments, soybean seeds (cultivar Conquista) were germinated in soil and grown in greenhouse conditions (avg. 21°C, max. 31°C, min. 15°C) under natural conditions of light, relative humidity 70%, and approximately equal day and night length. The first trifoliate leaves of three-week-old plants were excised and fed, via the petiole, solutions that induce the osmotic (10% PEG w/v) or ER stress responses (10 µg/ml tunicamycin or 50 mM AZC). After treatments for the times indicated in figure legends, the stressed trifoliate leaves and their untreated counterparts were immediately frozen in liquid N_2 and stored at -

80°C until use. Each stress treatment and RNA extraction were replicated in three independent experiments.

Generation of soybean microarrays

The microarray slides consisted of 5,760 amplified cDNA fragments from soybean libraries prepared from RNA of developing seeds (Thibaud-Nissen et al., 2003). ESTs from these libraries were placed into contigs to identify unigenes (Thibaud-Nissen et al., 2003), therefore a low redundancy in our set of clones is expected. The cloned cDNA fragments were amplified with M13 primers, purified using PCR Cleanup Filter Plates (Millipore, Bedford, MA), and eluted in water (according to the manufacturer's protocol). An aliquot of each amplified fragment reaction was separated through a 1% (w/v) agarose gel and visualized with ethidium bromide to assess size, quality and quantity. The purified PCR products were transferred to 384-well plates, and diluted with an equal volume of DMSO (Sigma). Finally, the PCR products were arrayed onto UltraGAPS slides (Corning, Corning, NY) using a 417TM Arrayer (Affymetrix, Santa Clara, CA), cross-linked by exposure to UV light at 250 mJ and baked at 75°C for 2 h.

Isoforms of the ER stress-related molecular chaperone BiP were amplified with gene-specific primers (Table S1) and included in the arrays. They consisted of three soybean isoforms A, C and D (Cascardo et al., 2000).

RNA extraction and labeled cDNA preparation

Total RNA was extracted from frozen leaves with TRIzol (Invitrogen, Carlsbad, CA) according to the instructions from the manufacturer, and further purified through silica columns. The quality and integrity of the RNA was monitored by spectrophotometry and agarose gel electrophoresis, respectively. For the microarray hybridizations, 10 µg of total RNA were reverse-transcribed with the SuperScriptTM Indirect cDNA Labeling System (Invitrogen) in the presence of cyanine-3-dUTP (Cy3-dUTP) or cyanine-5-dUTP (Cy5-dUTP; Amersham Biosciences, Piscataway, NJ) according to the manufacturer's instructions. RNA samples from each biological replicate were labeled twice, once with each dye, to control for dye-specific effects on the hybridizations.

For the real-time RT-PCR, 2 µg of total RNA were treated with DNase (Promega, Madison, WI) and fractionated through RNA purification columns (Qiagen, Valencia, CA). Reverse transcription was carried out using M-MLV reverse transcriptase (Invitrogen) and oligo-dT (18, IDT, Coralville, IA) primers (according to the protocol of the manufacturer). Prior to the real-time RT-PCR assays, the quality of the cDNA was assessed by PCR with gene-specific primers for ubiquitin associated protein (UBA; AW508375) to test for genomic DNA contamination, as these primers amplify a larger fragment size from genomic DNA than from cDNA.

Microarray hybridization, scanning and data analysis

Soybean cDNA microrrays were subjected to a similar hybridization protocol as described by (Hegde et al., 2000). Briefly, the microarray slides were incubated for 45 min in 50 ml of a pre-hybridization buffer 5X SSC, 0.1% (w/v) SDS and 1% (w/v) of BSA (all from Sigma), washed sequentially in ultra-pure water and iso(2)-Propanol (Fisher, Waltham, MA), and air-dried. Slides were then incubated with Cy3- and Cy5-labeled cDNA (20 µl) from treated and control samples for 20 h at 42°C in a water bath protected from light. The hybridization buffer consisted of 0.5% SDS (w/v), 5X SSC, 5X Denhardt's, 50% (v/v) formamide, 0.5 µg/µl denatured calf thymus DNA (all from Sigma) and 0.5 µg/µl polyA RNA (Amersham Biosciences). Following incubation, slides were washed sequentially in three steps in the following solutions: (1) 1X SSC, 0.2% (w/v) SDS, (2) 0.1X SSC, 0.2% (w/v) SDS, and (3) 0.1X SSC.

Microarray slides were scanned at the Cy3 (530 nm) and Cy5 (650 nm) wavelengths with a ScanArray 4000 laser fluorescent scanner (Packard Bioscience, Perkin Elmer, Wellesley, MA), at a laser power of 100% and photomultiplier tube (PMT) gain of 75%. The image analysis and calculation of mean background-subtracted intensity of the spots were performed using QuantArray software version 2.2 (PerkinElmer). Normalization based on the LOWESS algorithm (Yang et al., 2002) and data analysis were performed using Genespring software version 7.2 (Agilent Technologies, Santa Clara, CA).

Genes were considered differentially expressed if they met both of two criteria. The first was a fold change greater than 1.63 for PEG, 1.50 for TUN

and 1.46 for AZC. These values were calculated based on the mean of gene expression ratio for each treatment plus two standard deviations (expression ratio values above 2 were not included for this calculation). Second, the null hypothesis of the t-test [(mean of $\log_2$ratio)/SE] was rejected at 5% of probability. Additionally, genes with expression ratios higher than 2-fold in at least one technical replicate of each biological replicate were considered differentially expressed. A low stringency in our microarray data analysis was applied because relative expression of genes co-regulated by stress treatments was more accurately measured by real-time RT-PCR.

Annotations and Arabidopsis homologs of the soybean clones were assigned based on the top BlastX predictions against the GenBank (www.ncbi.nlm.nih.gov) and The Arabidopsis Genome Initiative databases (www.arabidopsis.org). For most of the corresponding proteins there is not a demonstrated biochemical function; therefore, we refer to them as “like” proteins.

Real-time RT-PCR data analysis

For the quantitative RT-PCR assays, sequences of cDNA and primers are listed in Table S1. Analysis of expression of calnexin, an ER-stress responsive gene, and seed maturation protein PM30, a drought-induced gene, were used as positive controls for the respective stress treatments.

To select an endogenous control gene for data normalization in real-time RT-PCR analysis, we analyzed three genes encoding histone H2A, 60S ribosomal protein L30, and RNA helicase, which had been chosen because

they had low and consistent expression ratios in the microarray results. The RNA helicase was used to normalize all values in the real-time RT-PCR assays, because it exhibited the lowest variation in expression values among treatments.

Real-time RT-PCR reactions were performed on an ABI7500 instrument (Applied Biosystems, Foster City, CA), using SYBR® Green PCR Master Mix (Applied Biosystems). The amplification reactions were performed as follows: 2 min at 50°C, 10 min at 95°C, and 40 cycles of 94°C for 15 sec and 60°C for 1 min. To confirm quality and primer specificity, we verified the size of amplification products after electrophoresis through a 1.5% agarose gel, and analyzed the Tm (melting temperature) of amplification products in a dissociation curve, performed by the ABI7500 instrument.

Fold variation in gene expression was quantified using the comparative Ct method: 2^-(ΔCtTreatment – ΔCtControl), which is based on the comparison of expression of the target gene (normalized to the endogenous control) between experimental and control samples.

Results

Using microarray slides containing amplified fragments of 5,760 soybean cDNAs, we conducted a broad survey to identify genes whose expression is affected by osmotic and ER stresses. In addition we expected to uncover any overlap in expression patterns that reflected integration of both stress-mediated signaling pathways. Three-week-old soybean plants were treated with either the ER-stress inducers AZC or tunicamycin, or the osmotic-stress inducer PEG (which led to a loss of water of around 60-70% in replicate plants). Within the microarray, we included, as positive controls, ER-stress induced molecular chaperone genes, such as the soybean BiP isoforms, A, C and D (Cascardo et al., 2000; 2001). Targets in the microarray slides were allowed to hybridize with pairs of Cy3- and Cy5-labeled cDNA probes from the following pairs of treated plants: tunicamycin and DMSO control, AZC and water control, PEG and water control. Two biological replicates and two technical replicates (dye-swap) were used for each treatment. The diagram shown in Figure 1 provides an overview of the microarray data showing the relative distribution of expression changes as shared and stress-specific responses.

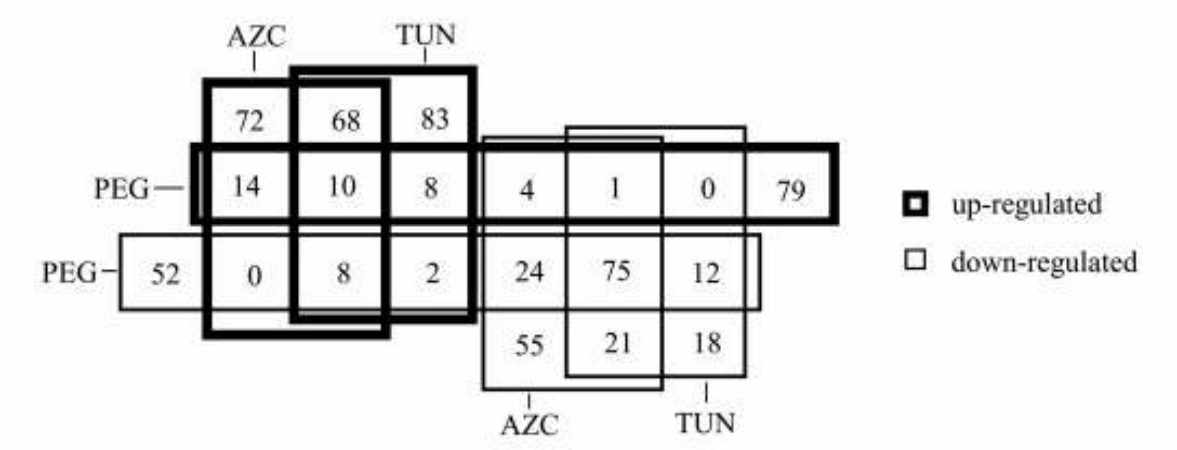

Figure 1. Venn diagram representing the distribution of specific and shared responses to TUN (10µg/ml, 24h), PEG (MW:8000 10%, 16h) and AZC (50mM, 16h) treatments, as determined by microarray analysis. Determination of differential expression is described in Material and Methods. Thick boxes represent up-regulation and thin boxes represent down-regulation.

ER stress-specific response

A total of 306 genes were differentially expressed in response to tunicamycin treatment, with 179 being up-regulated and 127 down-regulated (Figure 1). In response to AZC treatment, 352 genes were differentially expressed, 172 up-regulated and 180 down-regulated. To specifically target the UPR-regulated genes, we considered the overlapping genes that significantly responded to both tunicamycin and AZC treatments. This overlapping transcriptional response consisted of 183 genes, 86 up-regulated and 97 down-regulated (Figure 1, Tables S2 and S3).

Among the up-regulated genes, 17% represented genes of unknown functions. In the remaining set of genes for which some functional information

was available, those that exhibited an ER-stress response signature predominated (Table S2). More specifically, this up-regulated class of genes included those categorized as having a function in (i) protein folding (ii) ERAD and (iii) translational regulation. These results confirmed the activation of the ER-stress response pathway. In fact, the clones on the array with high homology to the known ER-resident molecular chaperones, BiP and calnexin, or the folding catalyst protein disulfide isomerase (PDI), were strongly up-regulated by both tunicamycin and AZC treatments (Figure 2).

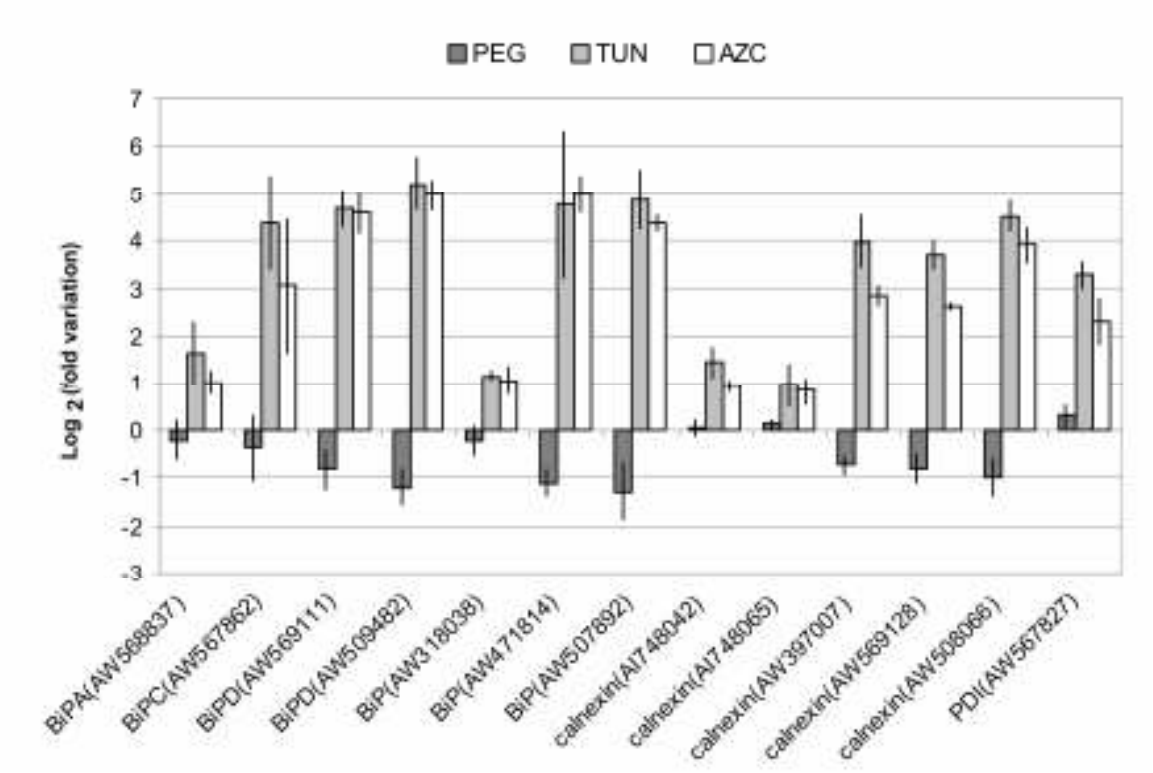

Figure 2. Effect of PEG, tunicamycin and AZC on the expression of *BiP*, *PDI* and calnexin genes (with accession numbers shown for each clone). The fold variation of gene expression (in relation to control treatment), as determined by microarray analysis, is presented in $\log_2$ scale (±SD, n=4 biological and technical replicates).

The expression of calnexin, an ER multi-functional protein involved in calcium homeostasis and protein folding, was used as a marker for ER-stress activation in a time-course experiment using real-time RT-PCR. Similar levels of induction of calnexin were observed between treatment with tunicamycin and AZC, possibly representing saturation in the expression (Figure 3A).

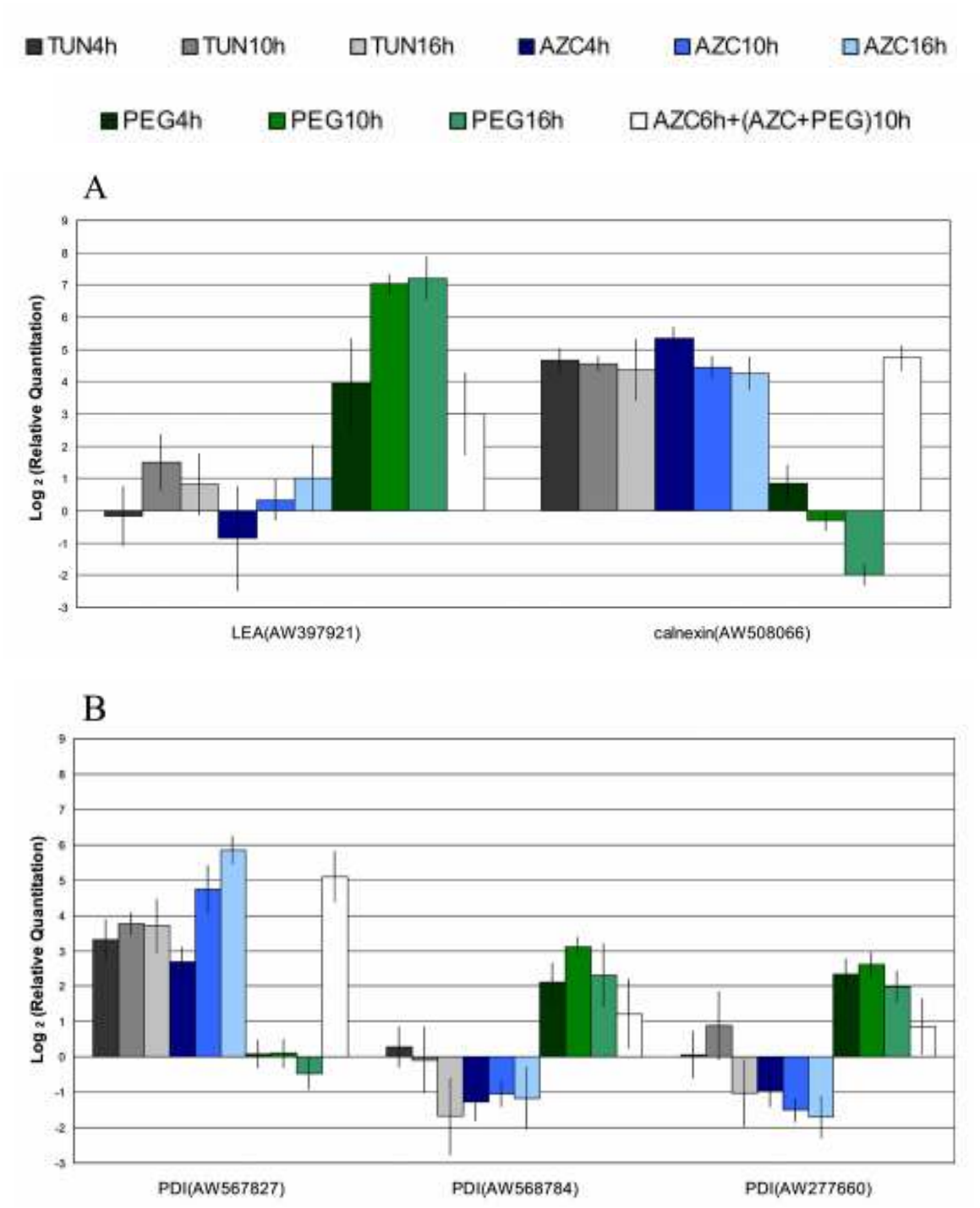

Figure 3. Time course of transcript induction by osmotic and ER stresses presented in $\log_2$ scale of gene expression, determined by real-time RT-PCR. Plants were treated with tunicamycin (gray), AZC (blue), PEG (green), or a combination of AZC and PEG (white) for the indicated period of time. A) Relative expression of representative genes of the response specific to ER (calnexin) or osmotic (SMP=LEA gene) stresses. B) Differential expression of the soybean PDI gene family members in response to tunicamycin and PEG treatments. GenBank Accession numbers are shown for each clone.

We found it particularly interesting that three cDNAs related to the PP2C and PP2A protein phosphatases were up-regulated by ER stress (Table S2, AW471739, AW569267, AW509424), as would be expected if they represented genes involved in UPR signaling in stressed cells. Accordingly, the *PP2C*-related cDNA is a homolog of the yeast PP2C (AAB64644) that regulates the UPR by dephosphorylation of Ire1 (Welihinda et al., 1998), a transmembrane protein kinase/endoribonuclease that triggers the UPR (Cox et al., 1993; Mori et al., 1993).

The identification of wheat MLO (transmembrane domain mildew resistance) allelic variants as endogenous substrates of an ERAD-related quality-control machinery provided direct evidence that an ERAD-like mechanism operates constitutively in plants (Muller et al., 2005). As part of the ER-stress response, the activation of this turnover mechanism has been observed in genome-wide analyses of *Arabidopsis* treated with inducers of ER stress and in a transcript-profiling assay of maize endosperm mutants that display a long-term ER stress response (Martinez and Chrispeels, 2003; Kamauchi et al., 2005; Kirst et al., 2005). Here we also observed a tunicamycin and AZC up-regulated repertoire of putative ERAD-related genes in soybean, such as those encoding polyubiquitin, ubiquitin conjugating enzyme, alpha subunit of the proteasome, CDC48 and Derlin (Table S2). These results further confirmed that, like in mammalian cells and in yeast, an ER stress-induced quality control mechanism in plants integrates the cellular response to conditions that alter protein folding in the ER.

During conditions of ER stress in mammals, a dynamic balance between the ER processing capacity and the protein synthesis rate is

adaptively achieved through a transient and general down-regulation of protein translation, as a component of the ER-stress response (Harding et al., 1999). The results of our microarrays were also effective in identifying a series of up-regulated genes related to ribosomal proteins (60S and 40S subunits; Table S2) that might represent regulatory elements in protein translation. Likewise, we found that a translational inhibitor protein (AW508686), a eukaryotic translation initiation factor 3 subunit 10 (AW317679), and a translation elongation factor 1-gamma (AI960794), which are potentially regulators of protein translation, were also responsive to ER stress. Collectively, the global transcriptional analysis of soybean cDNAs in response to ER stressors clearly unmasked the major branches of the conserved ER-stress response, arguing favorably for a good sampling of the genomic representation on our array and for the biological validation of the global analyses.

Osmotic stress-specific response

In response to osmotic stress caused by PEG treatment, a set of 116 up-regulated and 173 down-regulated genes was observed (Figure 1, Tables S4 and S5). Of particular interest were genes in two functional classes: genes directly involved in the stress response as cellular protectants, and regulatory genes involved in signaling events downstream of the osmotic stress response.

As representatives of the first class, we detected induction of LEA proteins, HSPs, senescence-related proteins, protease inhibitors, enzymes

associated with osmolyte distribution, such as sugar transporters, and in osmoprotectant biosynthesis, such as Δ1-pyrroline-5-carboxylate synthase (P5CS), which is involved in proline biosynthesis (Hu et al., 1992; Yoshiba et al., 1995), and sucrose synthase (Buchanan et al., 2005; Dejardin et al., 1999) (Table S4). Also in this category, we observed up-regulation of anti-oxidative defense components, such as glutathione peroxidase and glutathione-S-transferase homologs, which are involved in detoxification and protection from reactive oxygen species (Dixon et al., 1998; Edwards et al., 2000) and lipid transfer proteins that could possibly function in the stress-damaged membrane repair system, or in the regulation of cellular membrane permeability by changing the lipid composition in response to stress (Holmberg and Bulow, 1998; Torres-Schumann et al., 1992). As representatives of the second class, our microarray results detected the presence of two protein phosphatases, PP2C-like and PP1/PP2A PRL1-like coding cDNAs, and a serine/threonine-like protein kinase (Table S4). We also detected PEG-induced members of the NAC family of transcription factors. NAC proteins induced by dehydration have been previously described in *Arabidopsis* and rice (Fujita et al., 2004; Hu et al., 2006).

LEA genes were the most abundant among genes up-regulated by PEG treatment. We examined the osmotic stress response in more detail with real-time RT-PCR analysis of a gene encoding a putative LEA protein (Figure 3A). These data demonstrated that PEG treatment caused a gradual increase in induction of this *LEA* gene as a 15-fold increase in *LEA* mRNA level was detected at 4 h post-treatment, reaching 130- and 146-fold-changes at 10 h and 16 h, respectively. In contrast, the *LEA* gene did not

exhibit a significant variation of expression in response to ER-stress inducers and thus could be used as an appropriate monitor of the level of osmotic stress in treated plants.

The antagonistic response to ER stress and osmotic stress has an ER protein-folding signature

Different clones present in the soybean cDNA microarrays that likely encode ER-associated proteins, showed a differential and antagonistic regulation by ER and osmotic stresses. The most dramatic is within the PDI-like sequences where several family members were represented on the array. The protein disulfide isomerases (PDIs) belong to the superfamily of thioredoxin-domain-containing proteins that catalyze the formation of disulfide bonds and play an important role in protein folding. Within the TRX (thioredoxin) superfamily, they make a large gene family, designated *PDIL* (PDI-like proteins), encompassing disulfide isomerases and oxidoreductases that are associated predominantly with the protein secretory pathway in plants (Houston et al., 2005). The biochemically and genetically characterized members of this family were first identified in plants as ER-resident proteins that were induced under ER-stress conditions (Dorner et al., 1990). Based on sequence comparison, we identified in our soybean arrays four thioredoxin domain-encoding cDNA fragments that were classified as members of the PDIL family. Two clones were highly and specifically induced by both tunicamycin and AZC treatments, whereas two others were only induced by PEG (Tables S2 and S4). Analysis of gene expression using real-

time RT-PCR in a time-course experiment confirmed the differential regulation of the soybean PDIL gene family by osmotic and ER stresses and revealed that specific members of this family respond inversely to treatment with inducers of ER stress and PEG (Figure 3B). Sequence alignment and the expression pattern suggest to us that both PEG-induced clones refer to the same gene.

The finding that PEG treatment represses the tunicamycin-induced PDIL form extends to include other components of the ER protein processing machinery. An ATPase CDC48 homolog, *CDC48-like*, involved in ERAD was found to be up-regulated by ER-stress inducers, but repressed by PEG treatment (Table 1). Likewise, the *BiP* homolog clones as well as the PCR products of the soybean *BiP isoforms A, C* and *D* introduced in the arrays were inversely regulated by ER- and osmotic-stress (Figure 2). The cDNA homologs of the molecular chaperone calnexin were up-regulated by ER stress, but three calnexin cDNA fragments were significantly down-regulated by osmotic stress (Figure 2). We analyzed, by real-time RT-PCR, the kinetics of a calnexin homolog gene down-regulated by osmotic stress. The calnexin mRNA levels decreased gradually with the duration of treatment for 4, 10 and 16 h of exposure to PEG (Figure 3A). The general down-regulation of ER-molecular-chaperone genes by osmotic stress might reflect a general collapse and dysfunction of the ER under the severity of our PEG treatment rather than a specific biological phenomenon of gene regulation. To test this hypothesis we treated the soybean plants simultaneously with both PEG and AZC for 10 h and quantified the calnexin mRNA levels. Under PEG treatment, the ER stress agent AZC promoted calnexin induction to the same

extent as did either AZC or tunicamycin treatment alone (Figure 3A). Likewise, for the ER-stress-induced *PDI* (Figure 3B), the simultaneous treatment of PEG and AZC promoted the same level of gene induction as did the AZC treatment alone. These results clearly demonstrated that the ER is functioning and capable of signaling and activating the UPR under the PEG treatment conditions. Thus, the down-regulation of ER folding activities in response to osmotic stress may be a specific cellular response of plant cells.

Table 1. *Overlap of the ER stress and osmotic-stress transcriptional responses*

	Accession No. of Protein[a]	*e-value*[b]	Accession No. of Clone[c]	PEG[d]	*p-value*[e]	TUN[d]	*p-value*[e]	AZC[d]	*p-value*[e]
Genes induced by all of the treatments									
ATAF2 protein	BAC43493	8.E-31	AW459852	3.93	0.002	4.33	0.031	7.19	0.002
NAM protein	ABE79286	1.E-33	AW459732	2.81	0.008	3.31	0.019	5.27	0.001
N-rich protein	CAI44933	4.E-07	AI973541	2.76	0.005	3.39	0.009	4.33	0.012
N-rich protein	CAI44933	2.E-76	AW184865	1.93	0.008	2.14	0.012	2.42	0.003
ubiquitin-associated (UBA) protein	XP_466502	4.E-38	AW508375	3.05	0.000	3.12	0.024	2.59	0.014
eukaryotic translation initiation factor 5	P48724	2.E-65	AW472364	3.56	0.002	1.54	0.028	1.84	0.015
glutathione S-transferase	AAC18566	2.E-46	AW472161	3.83	0.003	3.19	0.002	2.75	0.002
glutathione S-transferase	AAG34800	1.E-48	AW397276	2.22	0.002	2.28	0.000	1.48	0.009
unknown			AW186110	2.58	0.005	3.17	0.003	9.56	0.000
unknown			AW508115	1.74	0.001	3.08	0.006	19.56	0.000
Genes repressed by all the treatments									
oxygen-evolving enhancer protein 1	P26320	3.E-39	AI941034	-3.27	0.000	-1.82	0.009	-3.07	0.001
thylakoid membrane phosphoprotein	NP_566086	1.E-21	AI960735	-1.93	0.004	-1.65	0.013	-2.03	0.011
NADPH-protochlorophyllide oxidoreductase	BAA21089	4.E-78	AW277941	-1.76	0.023	-2.08	0.009	-2.16	0.015
oxygen evolving enhancer protein	BAA96365	5.E-23	AW101019	-3.42	0.011	-2.24	0.001	-1.70	0.001
chlorophyll a/b-binding protein	CAA45523	4.E-75	AW397435	-9.07	0.001	-4.96	0.009	-7.02	0.000
chlorophyll a/b-binding protein	CAA45523	1.E-75	AW101657	-5.56	0.010	-2.38	0.015	-2.06	0.003
chlorophyll a/b-binding protein CP24	AAD27882	3.E-41	AI736217	-7.54	0.000	-5.72	0.003	-10.78	0.001
chlorophyll a/b binding protein type II	AAL29886	3.E-18	AI736285	-7.45	0.006	-3.69	0.048	-10.00	0.000
chlorophyll a/b binding protein	AAD27877	9.E-85	AW397809	-15.20	0.001	-10.48	0.004	-38.20	0.000
chlorophyll a-b binding protein	P13869	2.E-85	AW471940	-5.19	0.005	-4.23	0.016	-8.21	0.001
RuBisCO small subunit 1	CAA23736	7.E-53	AW278725	-4.74	0.003	-5.01	0.107	-58.93	0.000
chlorophyll a/b-binding protein	AAA50172	1.E-64	AW472492	-28.79	0.002	-10.26	0.028	-31.02	0.000
oxygen-evolving enhancer protein 1	P26320	8.E-64	AW567782	-2.11	0.030	-1.65	0.050	-1.58	0.005
chlorophyll a/b-binding protein CP24	AAD27882	2.E-75	AW568341	-9.95	0.005	-6.83	0.004	-16.75	0.000
putative chlorophyll a/b-binding protein	XP_482572	2.E-73	AW568620	-11.01	0.004	-6.02	0.004	-8.13	0.000
oxygen evolving enhancer protein	BAA96365	9.E-67	AW568090	-3.99	0.014	-4.53	0.037	-14.93	0.000
type II chlorophyll a/b binding protein	CAA57492	1.E-78	AW100823	-3.61	0.000	-2.93	0.024	-9.04	0.001
chlorophyll a/b-binding protein type I	AAQ54512	1.E-36	AW100631	-5.39	0.000	-2.70	0.006	-3.23	0.004
chlorophyll a/b-binding protein type III	S04125	2.E-43	AI794678	-7.95	0.000	-3.36	0.037	-10.81	0.000
chlorophyll a/b binding protein	AAD27877	2.E-22	AW508739	-7.35	0.006	-3.23	0.007	-2.99	0.003
chlorophyll a/b-binding protein CP24	AAD27882	8.E-72	AW568252	-7.94	0.011	-3.40	0.002	-3.53	0.000
chlorophyll a/b-binding protein CP24	AAD27882	6.E-88	AW570380	-5.53	0.001	-5.23	0.012	-10.41	0.002
photosystem I subunit X precursor	AAL32043	4.E-46	AW277960	-4.65	0.014	-3.72	0.009	-4.81	0.000
oxygen-evolving enhancer protein 1	P14226	4.E-71	AW472001	-4.74	0.005	-3.13	0.028	-5.54	0.000
photosystem I psaH protein	AAQ21121	3.E-53	AW471851	-3.39	0.003	-2.98	0.002	-4.82	0.002
chlorophyll a/b binding protein	AAD27877	6.E-29	AW472547	-9.06	0.001	-3.54	0.019	-1.62	0.004
photosystem II reaction center W protein	CAA59409	1.E-28	AW471847	-2.55	0.015	-1.74	0.024	-1.49	0.002
photosystem II protein	AAM61462	6.E-07	AW508451	-4.91	0.009	-2.91	0.003	-1.72	0.004
photosystem I reaction center subunit III	AAD27880	1.E-82	AW508794	-5.25	0.002	-4.83	0.030	-33.31	0.000
geranylgeranyl hydrogenase	AAD28640	9.E-48	AW185978	-2.18	0.014	-1.89	0.003	-2.37	0.010
ultraviolet-B-repressible protein	AAS58469	1.E-29	AW317705	-5.24	0.003	-4.16	0.011	-10.16	0.000
glutamine synthetase precursor	AAK43833	4.E-66	AI736144	-2.28	0.010	-2.17	0.007	-2.19	0.010
myo-inositol-1-phosphate synthase	AAK72098	7.E-95	AI941146	-2.30	0.001	-1.71	0.011	-2.30	0.006
UDP-glucose 4-epimerase	Q43070	4.E-83	AI856802	-3.52	0.001	-2.64	0.001	-3.32	0.007
putative auxin-amidohydrolase precursor	CAG32961	1.E-18	AW278733	-4.23	0.001	-3.33	0.007	-8.72	0.000
granule-bound starch synthase Ib precursor	BAC76613	5.E-49	AW508018	-1.67	0.004	-2.21	0.031	-2.16	0.006
selenium binding protein	CAC67501	6.E-50	AW101647	-4.82	0.008	-4.94	0.021	-28.20	0.000
ATP-dependent helicase	NP_850847	1.E-58	AW570395	-3.97	0.003	-5.72	0.016	-12.70	0.000
microsomal omega-3 fatty acid desaturase	BAC87757	1.E-86	AI960953	-1.70	0.009	-1.71	0.012	-3.54	0.000
granule-bound starch synthase Ib precursor	BAC76613	4.E-65	AW472193	-7.20	0.008	-6.51	0.000	-17.58	0.000
carboxylic ester hydrolase	NP_177281	2.E-51	AW278929	-2.16	0.038	-3.73	0.023	-2.30	0.010
cinnamoyl-CoA reductase	AAY86360	5.E-60	AW508388	-3.11	0.007	-4.27	0.004	-5.60	0.000
transformer-SR ribonucleoprotein	CAA70700	3.E-38	AW568037	-3.07	0.011	-2.82	0.000	-7.39	0.000
putative cinnamoyl-CoA reductase	AAT39306	2.E-16	AW101559	-2.91	0.004	-3.01	0.005	-1.68	0.010
myo inositol 1-phosphate synthase	CAJ15162	5.E-56	AW100674	-4.42	0.000	-4.48	0.003	-5.52	0.001
aldose 1-epimerase-like protein	NP_566594	3.E-66	AW507799	-2.36	0.009	-2.74	0.012	-2.26	0.000
ACT domain-containing protein	NP_565908	5.E-35	AW508692	-2.57	0.032	-1.75	0.002	-1.58	0.043
cytochrome P450 monooxygenase	AAD38930	8.E-55	AW507877	-1.86	0.009	-3.74	0.017	-2.98	0.027

Table 1. *(Continued from previous page.)*

	Accession No. of Protein[a]	*e-value*[b]	Accession No. of Clone[c]	PEG[d]	*p-value*[e]	TUN[d]	*p-value*[e]	AZC[d]	*p-value*[e]
palmitoyl-acyl carrier protein thioesterase	AAD01982	3.E-25	AW568268	-2.58	0.039	-1.71	0.021	-5.28	0.001
1-aminocyclopropane-1-carboxylate oxidase	AAX84675	3.E-86	AW508290	-6.79	0.010	-5.34	0.020	-11.62	0.000
plasma membrane polypeptide	CAB61742	1.E-40	AW459777	-1.83	0.028	-2.05	0.005	-1.67	0.016
acid phosphatase	CAA11075	8.E-20	AI930921	-3.69	0.000	-2.61	0.016	-4.07	0.001
ATP synthase gamma chain	CAA45150	5.E-80	AW186038	-4.15	0.002	-2.71	0.010	-5.77	0.000
putative leukotriene-A4 hydrolase	AAM91766	3.E-50	AW277270	-2.08	0.025	-1.67	0.019	-1.88	0.004
ATP synthase B' chain	CAA50520	4.E-24	AW471917	-2.94	0.008	-3.25	0.013	-7.91	0.001
granule-bound starch synthase Ib precursor	BAC76613	8.E-78	AW472190	-4.85	0.005	-5.28	0.001	-8.47	0.000
pepsin A	NP_196320	4.E-54	AW568189	-5.01	0.024	-2.34	0.003	-4.01	0.004
plastid ribosomal protein CS17	CAA77502	4.E-32	AW508645	-2.47	0.008	-2.16	0.005	-4.58	0.000
phosphoglycerate kinase	AAF85975	2.E-18	AW568791	-3.08	0.012	-2.44	0.009	-6.98	0.000
chitinase-like protein	BAC81645	1.E-38	AW508700	-2.20	0.015	-2.45	0.007	-2.81	0.001
unknown			AW508640	-1.80	0.017	-2.27	0.015	-1.61	0.033
unknown			AW570244	-2.03	0.004	-1.97	0.001	-2.81	0.001
unknown			AW598111	-2.16	0.005	-1.58	0.009	-2.58	0.013
unknown			AW508120	-4.73	0.001	-4.19	0.043	-19.62	0.000
unknown			AW100867	-2.40	0.007	-2.00	0.001	-1.65	0.016
unknown			AI941196	-1.85	0.003	-2.17	0.013	-2.01	0.000
unknown			AW164582	-1.64	0.006	-2.00	0.007	-3.58	0.001
unknown			AW471578	-2.03	0.025	-2.13	0.003	-3.51	0.000
unknown			AW508445	-3.28	0.008	-2.41	0.031	-1.67	0.020
unknown			AW507853	-3.02	0.014	-2.91	0.005	-6.71	0.000
unknown			AW569116	-3.17	0.002	-2.02	0.008	-1.47	0.038
unknown			AW471729	-2.02	0.037	-3.36	0.009	-2.07	0.008
unknown			AW568035	-10.74	0.006	-2.49	0.047	-1.79	0.001
unknown			AW101065	-3.07	0.008	-3.62	0.006	-3.41	0.033
unknown			AW568660	-6.56	0.002	-2.69	0.002	-3.33	0.000
Genes induced by TUN and AZC but repressed by PEG									
CDC48-like protein	AAP53974	5.E-71	AW509037	-1.70	0.009	10.57	0.000	5.78	0.001
calnexin homolog precursor	BAD81043	9.E-78	AW569128	-1.76	0.044	12.82	0.000	6.09	0.000
calnexin homolog precursor	Q39817	9.E-59	AW397007	-1.67	0.005	15.69	0.001	7.16	0.000
calnexin homolog precursor	Q39817	1.E-82	AW508066	-2.00	0.015	22.76	0.000	15.03	0.000
BiP isoform D			AW569111	-1.78	0.029	25.60	0.000	23.72	0.000
BiP isoform D	AAK21920	3.E-101	AW509482	-2.30	0.008	37.13	0.000	31.41	0.000
BiP	BAD95470	1.E-76	AW471814	-2.16	0.023	27.22	0.034	31.90	0.000
BiP	BAD95470	5.E-68	AW507892	-2.43	0.022	29.42	0.001	20.75	0.000
Genes repressed by TUN and AZC but induced by PEG									
unknown			AW186103	1.74	0.003	-1.77	0.049	-1.72	0.005

[a] Protein annotations obtained from BlastX using cDNA clone sequence against GenBank. [b] Expected values obtained by BlastX. [c] Clone accession number in the GenBank. [d] Fold variation in gene expression converted from means of the $\log_2$ratio (treated/control channel) from plants treated with PEG, TUN or AZC and their respective controls. [e] probability values obtained from the *t-test*.

Modest overlap of the ER-stress and osmotic-stress transcriptional responses

An overlap of the osmotic-stress and the ER-stress responses is represented by 10 up-regulated genes, 75 down-regulated genes, 8 ER stress-induced but osmotically repressed genes, and 1 osmotically stress-induced but ER stress-repressed gene (Figure 1, Table 1). Thus, only about 10% of the genes up-regulated by either ER or osmotic stress in our survey population were induced by both treatments. In contrast, a substantial overlap in the genes down-regulated by ER and osmotic stresses was observed, with about 50% and 75% of the genes being in the sets affected by osmotic stress and ER stress, respectively. These results represent a much larger down-regulation of transcripts by ER stress than those reported previously (Martinez and Chrispeels, 2003; Kamauchi et al., 2005; Tables S3 and S7). Likely, these results reflect substantial differences in experimental design and conditions, including cDNA library origin, plant background, stringency of stress conditions, plant species, setting up and processing of microarrays.

While 25% of the repressed genes that were ER-stress specific were predicted to be related to the secretory pathway (Table S3), the remaining 75% were co-repressed genes that seem to represent a general response of plants to abiotic stresses, as they reflect an inhibition of photosynthesis and development. In fact, a common effect of osmotic and ER stresses revealed by the microarray analysis was a general decrease in the expression of photosynthesis-related genes, including genes that encode the oxygen-evolving enhancer protein, chlorophyll a/b binding protein, small subunit of

RuBisCO, NADPH-protochlorophyllide oxidoreductase (involved in chlorophyll biosysnthesis), a thylakoid membrane phosphoprotein and others. There are at least 32 redundant clones involved in photosynthesis that are down-regulated by all three treatments (Table 1). Consistent with photosynthesic inhibition was our observation of three starch synthase homolog cDNAs, and two clones related to cinnamoyl-CoA reductase, a lignin synthesis-related gene being repressed by both stresses (Table 1). Another class represented in the co-repressed category included members involved in hormone biosynthetic pathways, such as 1-aminocyclopropane-1-carboxylate oxidase (*ACC*, AW508290), involved in ethylene biosynthesis (Dong et al., 1992), an IAA-amino acid conjugate hydrolase (AW278733), which regulates the level of the auxin indole-3-acetic acid (IAA; LeClere et al., 2002)), geranylgeranyl hydrogenase and cytochrome P450 monooxygenase that participate in the gibberellin (GAs) biosynthetic pathway (Winkler and Helentjaris, 1995; MacMillan, 1997).

The overlap in genes that shared the up-regulated response revealed two cDNA fragments that encode putative transcription factors belonging to the NAM family (NAC and ATAF2 homologs), two clones that encode DCD-domain-containing proteins (N-rich proteins), two encoding glutathione-S-transferase, a *UBA* protein gene, an eukaryotic translation initiation factor 5 (*eIF5*) gene and two cDNAs whose function is unknown (Table 1). A more precise analysis using real-time RT-PCR confirmed a significant induction of co-up-regulated transcripts by tunicamycin, AZC or PEG treatment (Figure 4).

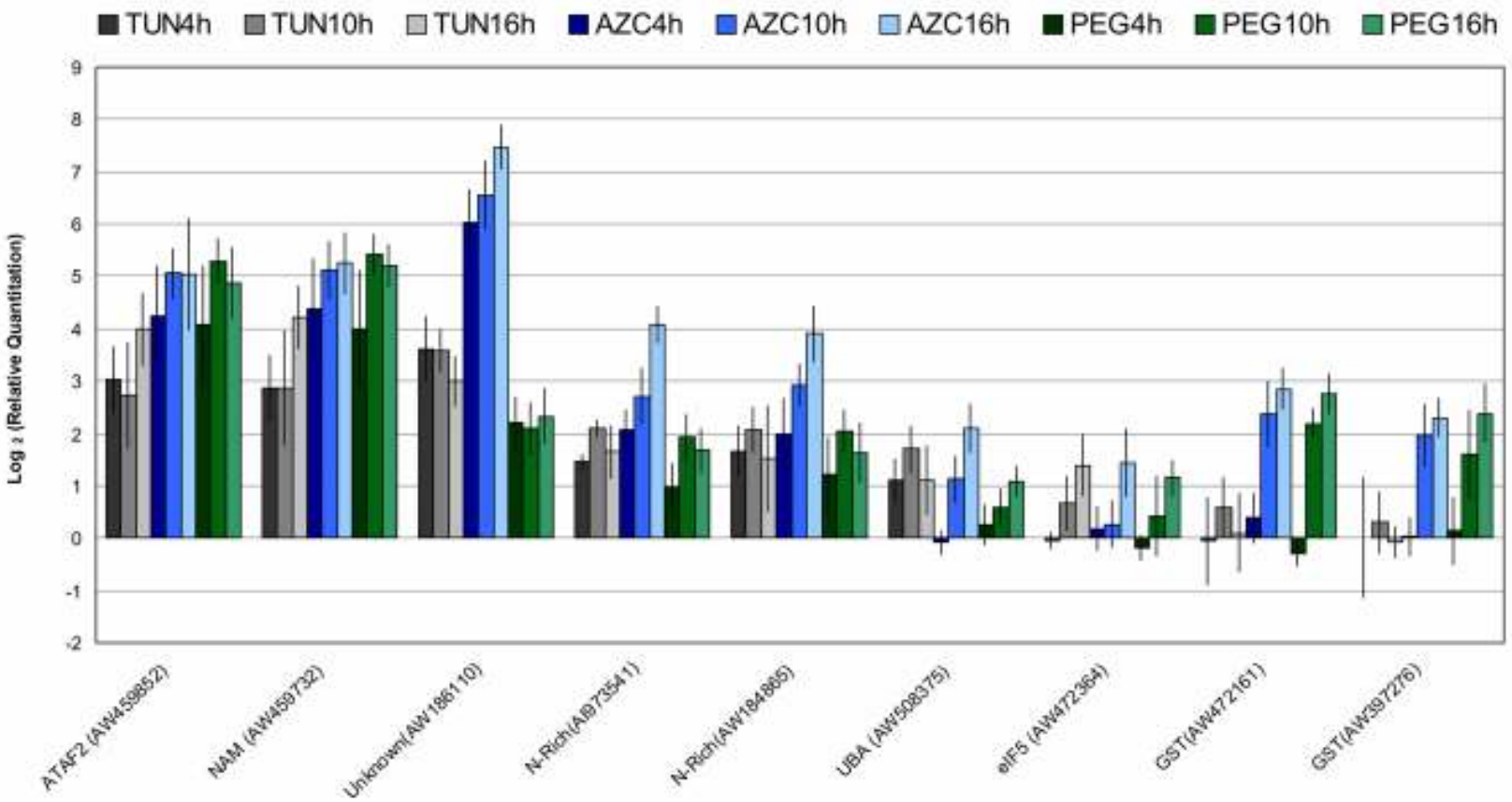

Figure 4. Time course of transcript induction of the co-up-regulated genes by tunicamycin, AZC and PEG treatments. The fold variation (±SD, n=3 biological replicates) showed in $\log_2$ scale of gene expression was determined by real-time RT-PCR, from plants treated with tunicamycin (gray), AZC (blue), or PEG (green), for the indicated period of time. GenBank Accession numbers of certain clones are presented to help clone identification.

If these genes had a role in regulating this branch of the pathway, they would be predicted to be induced early. We tested this possibility with a time-course experiment. Real-time RT-PCR assays during induction demonstrated that the *NAC*-containing proteins *ATAF2* and *NAM* exhibited an early kinetics of induction, consistent with their putative role as transcriptional factors (Figure 4). Four-hour treatments were sufficient to saturate their expression, which remained high for the duration of the experiment. A similar kinetic pattern was observed for the *N-rich* DCD-domain transcripts AI973541 and AW184865, which were strongly induced at 4 h and reached maximum accumulation at 10 h post treatment. Accordingly, the *N-rich* (AW184865) gene has been shown to be rapidly induced during the hypersensitive response in soybean (Ludwig and Tenhaken, 2001). In contrast to the early induction of the *NAC* and *N-rich* related genes by ER and osmotic stresses, the induction of the remaining co-up-regulated genes occurred with delayed kinetics (Figure 4). The induction of the *UBA*, *eIF5*, *GST* (AW472161) and *GST* (AW397276) transcripts was initially detected by 10 h post-treatment and continued to increase through the 16 h time point. The kinetic pattern of the co-up-regulated genes clearly defined a class of early response genes that may have regulatory functions and delayed genes that may exhibit protective functions.

To examine directly the interactions of ER and osmotic stress on the co-up-regulated response, we analyzed whether the combination of AZC and PEG treatments promoted an additive increase in expression (Figures 5A and 5B). Seven of the nine co-induced genes that we examined (asterisks) were induced by both stimuli in a more than additive fashion. Thus, the ER-

stress and osmotic-stress signaling responses are integrated in a synergistic, convergent manner at the gene activation level.

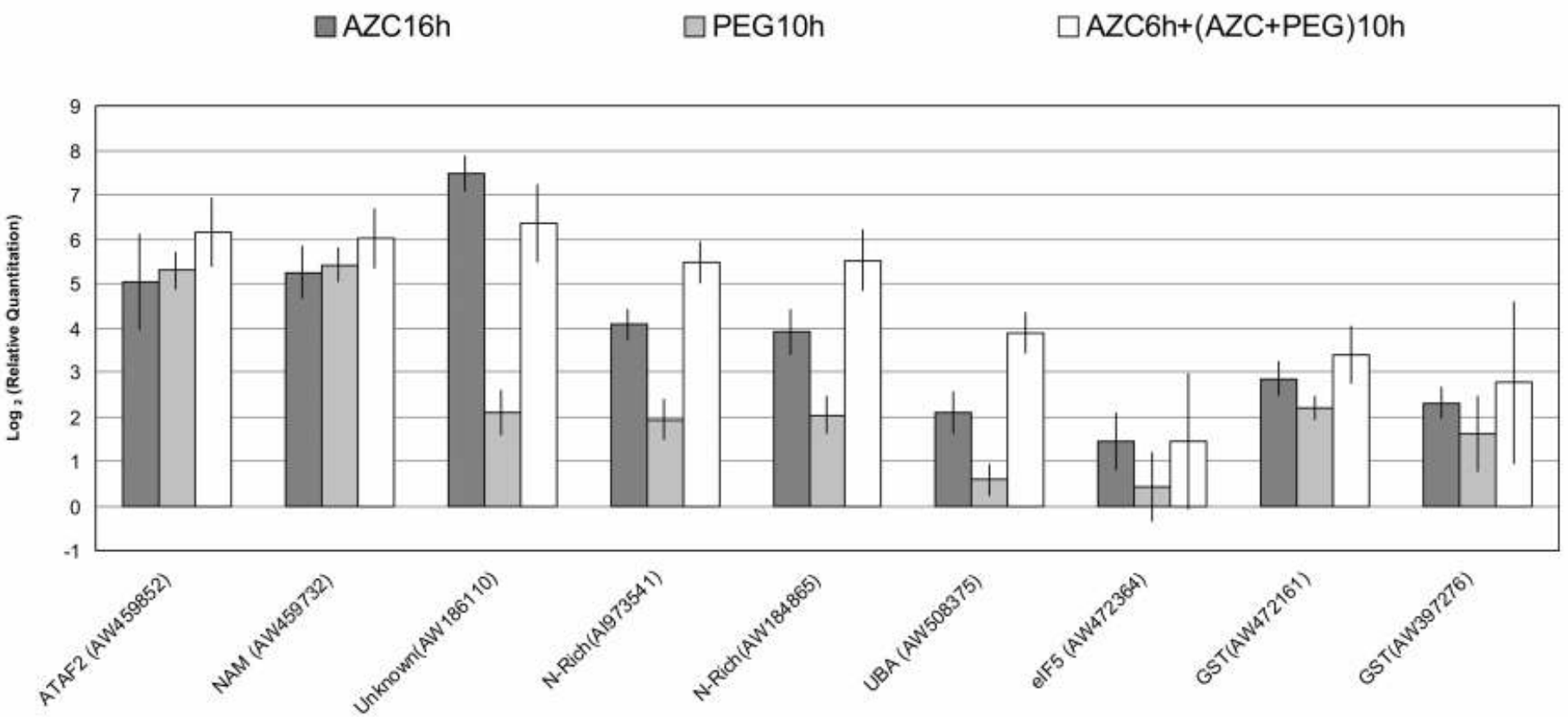

Figure 5. Synergistic induction of gene expression by the combination of PEG and AZC treatments, determined by real-time RT-PCR. The plants were treated for 6 hours with AZC only, and then 10 hours with a combination of AZC and PEG. Values for AZC 6h+(AZC+PEG)10h are relative to H_2O control treatment for 16 hours (±SD, n=3 biological replicates).

Discussion

Using a cDNA microarray potentially representing approximately 5,700 soybean gene tags, our expression profiling in response to ER stress and osmotic stress provided an unprecedented view of the overlapping transcriptional responses to ER stress and osmotic signaling. However, in searching for crosstalk between these two signaling pathways, we detected a much larger change for the UPR-regulated transcripts than was reported in Arabidopsis (Martinez and Chrispeels, 2003; Kamauchi et al., 2005). Given that a plant is constantly adapting to its environment and its physiological status will impact the overall response to stress (Kreps et al., 2002), one may consider that some of the changes reported here are associated with specific conditions of our experimental design. For instance, to induce ER stress both AZC and tunicamycin were directly taken up through the cut petiole of young soybean plants and vascularly translocated to their leaves. Excision of the petiole would not be expected to elicit a wound response (Reymond et al., 2000) and any effects due to tissue treatments would be accounted for by inclusion of untreated cut petiole controls to prevent wounding-specific changes from being included as variation in ER-stress responses. To extend the candidate gene list of the overlapping ER-stress and osmotic signal responses, we used a relative low stringency cutoff criterion for variation in expression (close to a 2-fold change in expression level). Additionally, we used an experimental design based on two-biological plus two-technical replicates to minimize detection of random and technical variations. The validity of the approach was supported by the fact that our results revealed the major branches of the ER-stress response as well as the major

osmotically regulated changes reported in other surveys (Kreps et al., 2002; Seki et al., 2002; Denekamp and Smeekens, 2003; Martinez and Chrispeels, 2003; Kamauchi et al., 2005). In addition, the coordinate induction of a subset of genes by both ER and osmotic stresses was confirmed by real time RT-PCR (Figure 4).

Our results indicated that genes encoding ER chaperones and folding catalysts, such as BiP, calnexin and PDI, were antagonistically affected by the PEG-induced osmotic signal and activation of the UPR. While the UPR-mediated up-regulation of the ER molecular chaperones is a conserved feature in eukaryotic cells (for review see Ma and Hendershot, 2004), coordinate down-regulation of these proteins by PEG-induced dehydration has not been previously described. In fact, previous studies describing drought- or osmotic-stress responses have focused on just a small subset of ER molecular chaperones. For instance, in spinach, drought stress has been shown to reduce the BiP mRNA level, whereas in soybean and tobacco, a subset of BiP transcripts has been shown to be up-regulated by PEG-induced osmotic stress, water deficit or ABA treatment (Anderson et al., 1994; Denecke et al., 1995; Cascardo et al., 2000; Alvim et al., 2001). The apparent contradiction of these results has been explained as a function of the plant background in which the BiP basal level and the cellular secretory activity would signal the necessity of BiP up- or down-regulation under drought. More recently, genomic scale information on stress-induced changes has allowed a more in-depth view of the scenario for reprogramming plant gene expression as the result of interaction of the plant with the environment. A recent wide-genomic analysis of PEG-specific changes in

maize clearly demonstrated that a large fraction of down-regulated transcripts are represented by protein biosynthesis-related genes (Jia et al., 2006). These results are not surprising as PEG-induced cellular dehydration is expected to slow down protein synthesis. Under these conditions, a repression of ER folding activities by the osmotic signal would permit the ER protein processing capacity to be balanced with the low rate of protein synthesis. Our results showing a coordinate down-regulation of ER molecular chaperones in response to PEG treatment fit quite well with this current model of coupling ER protein processing capacity to the rate of protein synthesis (Bernales et al., 2006). However, whether the decrease in the ER protein processing capacity is a primary response to the osmotic signal or a consequence of the limitation in the overall protein synthesis rate under cellular dehydration remains to be determined.

The present ER-stress- and osmotic-stress-induced transcriptional studies demonstrate a clear predominance of stimulus-specific positive changes over the shared response (5.5% of the total up-regulated genes). This scenario indicates that PEG-induced cellular dehydration and ER stress elicited very different up-regulated responses within a 10-h stress treatment regime. In contrast, we observed a much larger overlap of the down-regulated response. From the 195 clones significantly down-regulated in the microarray analysis, 75 cDNAs (38%) were found to be down-regulated by all the stress treatments. These possibly represent a general stress response. In fact, a large fraction of the genes down-regulated in all treatments consist of photosynthesis-related genes, such as chlorophyll a/b binding protein, components of photosystems I and II and the small subunit of RUBISCO, as

well as genes associated with development, for example, those encoding enzymes involved in hormone biosynthetic pathways. Recently, a cDNA microarray analysis revealed that photosynthesis-related genes were down-regulated by PEG treatment of maize seedlings (Jia et al., 2006). Likewise, similar studies in other plant species have demonstrated that inhibition of photosynthesis is a common general response to drought, cold, high salinity and ABA (Fowler and Thomashow, 2002; Seki et al., 2002).

Our data provide evidence that the up-regulated response common to all treatments was indeed an integrated pathway reflecting crosstalk between the UPR and osmotic stress signaling. A combination of the ER stress- and osmotic stress-induced treatments promoted a synergistic effect on the induction level of the common up-regulated genes although to a different extent for various genes (Figure 5, asterisks). These results indicate that information transfer between the signaling pathways occurs through the shared, integrated response with the potential to alter or to intensify the output of the different pathways. Furthermore, they suggest that the ER stress and osmotic signaling pathways are likely to converge on the co-regulated target genes at the level of gene activation. Based on these observations, we considered as components of the integrated pathway only the subset of the co-regulated genes that were synergistically induced by the simultaneous treatment of the soybean plants with AZC and PEG (Figures 5A and 5B, asterisks). Comparison of the overlapping positive responses at different time points classified the integrative genes as having early or delayed effects. The early genes include the homolog cDNAs for ATAF2 and NAM, which belong to the NAC gene family of trans-acting factors (for review

see Olsen et al., 2005). Several members of this family of plant specific DNA-binding proteins have been shown to exhibit transcriptional activation (Xie et al., 2000; Duval et al., 2002; Fujita et al., 2004; Tran et al., 2004; Hu et al., 2006). The delayed genes consisted of functional genes which may exhibit cytoprotective properties, such as UBA (ubiquitin-associated) domain protein, possibly involved in the ubiquitin pathway. Likewise, a GST (glutathione-S-transferase) cDNA was coordinately induced by both stresses with delayed kinetics. Osmotic and ER stresses are known to generate reactive oxygen species that trigger the induction of the antioxidant system (Sgherri et al., 1993; Mittler and Zilinskas, 1994; Harding et al., 2003).These results provide a critical framework for future studies on the elucidation of the pathways integrating ER stress and osmotic signals.

With respect to the underlying mechanism of BiP-mediated increases in water deficit tolerance that provided the foundation for pursuing these studies, the results of the microarray analysis highlighted relevant insights. The observed PEG-mediated down-regulation of ER molecular chaperones may imply that, unlike tunicamycin, PEG treatment does not cause protein misfolding in the ER. This finding argues against the need to maximize the ER protein processing capacity for cellular recovery from the osmotic stress. Therefore, under the PEG-induced stress conditions of our experiments, which mimic drought stress in soybean, an ectopic increase of ER molecular chaperone activities per se could not counteract the global deleterious effects of the osmotic stress. In view of these observations, it is reasonable to assume that the protective role of BiP against water dehydration may not be associated with its molecular chaperone activity, but rather it may be linked to

its regulatory role as a sensor of the ER stress signal (Bertolotti et al., 2000; Shen et al., 2002). Like in mammalian cells, the induction of BiP in plants has been shown to block ER stress signals (Leborgne-Castel et al., 1999). How might a block in the ER stress signal by high BiP concentrations affect osmotic signaling? The finding that these signaling pathways converge upon the integrative genes to potentiate the cellular response provides the molecular link that would permit the flow of the integrated information to be controlled by a regulator of either one of the stress signals. Additional experiments will be required to elucidate the physiological consequences of activation of the integrated pathway and to determine how or if manipulation of BiP levels might affect the response.

The integrative genes, such as ATAF2 homolog and the N-rich genes, have been linked to the pathogen response and programmed cell death (PCD; Delessert et al., 2005; Tenhaken et al., 2005). Overexpression of the Arabidopsis ATAF2 gene in transgenic lines led to repression of a number of pathogenesis-related protein genes, whereas their levels were increased in ATAF2 knock-out lines (Delessert et al., 2005). ATAF2 belongs to the NAC gene family that is represented by 109 members in the Arabidopsis genome (Riechmann et al., 2000) and 20 of these are present in the leaf senescence dbEST (Guo et al., 2004). Additionally, many groups have reported expression of NAC genes in senescing leaves (John et al., 1997; Andersson et al., 2004; Guo et al., 2004; Lin and Wu, 2004; Buchanan-Wollaston et al., 2005) and a NAC transcription factor (NAM-B1) isolated from wheat has been shown to regulate leaf senescence (Uauy et al., 2006). As for the N-rich genes, they encode a DCD (development and cell death) domain which is

thought to be involved in the hypersensitive response and programmed cell death (Ludwig and Tenhaken, 2001; Tenhaken et al., 2005). Based on the putative roles of the integrative genes, the possibility that the integrated pathway might transduce a PCD signal generated by prolonged ER stress and osmotic stress warrants further investigation.

Major Conclusions

- Our data reveal overlapping in transcriptional profiles and suggest integration between ER- and osmotic-stress pathways
- The divergence in the regulation of molecular chaperones and the ERAD component CDC48, and the diversity in function of members of the PDI family in response to ER- and osmotic-stress reveal a complex regulatory mechanism in stress responses.
- The list of genes commonly regulated by stress responses provides new possibilities for obtaining plants tolerant to drought.
- The transcriptional analysis of soybean cDNAs in response to ER- and osmotic-stress covered main components of these stress responses, demonstrating a good partial genomic representation of the cDNA population in our arrays.
- The validation and reproduction of the microarrays data by real-time RT-PCR demonstrate accuracy in the microarray analysis and criteria for differential expression.

References

Almoguera C, Jordano J (1992) Developmental and environmental concurrent expression of sunflower dry-seed-stored low-molecular-weight heat-shock protein and Lea messenger-rnas. *Plant Mol. Biol.* **19,** 781-792.

Alvim, F.C., Carolino, S.M.B., Cascardo, J.C.M., Nunes, C.C., Martinez, .C.A, Otoni W.C. and Fontes, E.P.B. (2001) Enhanced accumulation of BiP in transgenic plants confers tolerance to water stress. *Plant Physiol.* **126,** 1042-1054.

Anderson, J.V., Li, Q.B., Haskell, D.W. and Guy, C.L. (1994) Structural organization of the spinach endoplasmic reticulum-luminal 70-kilodalton heat-shock cognate gene and expression of 70-kilodalton heat-shock genes during cold-acclimation. *Plant Physiol.* **104,** 1359-1370.

Andersson, A., Keskitalo, J., Sjodin, A. et al. (2004) A transcriptional timetable of autumn senescence. *Genome Biol.* **5,** R24**.**

Apse, M., Aharon, G., Snedden, W. and Blumwald, E. (1999) Salt tolerance conferred by overexpression of a vacuolar Na+/H+ antiport in *Arabidopsis*. *Science* **285,** 1256-1258.

Badawi, G.H., Yamauchi, Y., Shimada, E., Sasaki, R., Kawano, N., Tanaka, .K., Tanaka, K. (2004) Enhanced tolerance to salt stress and water deficit by overexpressing superoxide dismutase in tobacco (Nicotiana tabacum) chloroplasts. *Plant Sci.* **166,** 919-928.

Bartels, D, (2001) Targeting detoxification pathways: an efficient approach to obtain plants with multiple stress tolerance? *Trends Plant. Sci.* **6,** 284-286.

Bernales, S., Papa, F.R. and Walter, P. (2006) Intracellular Signaling by the Unfolded Protein Response. *Ann. Rev. Cell Dev. Biol*. **22,** 487-508.

Bertolotti, A., Zhang, Y.H., Hendershot, L.M., Harding, H.P. and Ron, D. (2000) Dynamic interaction of BiP and ER stress transducers in the unfolded-protein response. *Nat. Cell Biol.* **2,** 326-332.

Buchanan-Wollaston, V., Page, T., Harrison, E., Breeze, E., Lim, P.O., Nam, H.G., Lin, J.F., Wu, S.H., Swidzinski, J., Ishizaki, K. and Leaver, C.J. (2005) Comparative transcriptome analysis reveals significant differences in gene expression and signalling pathways between developmental and dark/starvation-induced senescence in Arabidopsis. *Plant J.* **42,** 567-585.

Buchanan, C.D., Lim, S.Y., Salzman, R.A., Kagiampakis, L., Morishige, D.T., Weers, B.D., Klein, R.R., Pratt, L.H., Cordonnier-Pratt, M.M., Klein, P.E. and Mullet, J.E. (2005) Sorghum bicolor's transcriptome response to dehydration, high salinity and ABA. *Plant Mol. Biol.* **58,** 699-720.

Calfon M, Zeng HQ, Urano F, Till JH, Hubbard SR, Harding HP, Clark SG, Ron D (2002) IRE1 couples endoplasmic reticulum load to secretory capacity by processing the XBP-1 mRNA. *Nature* **415,** 92-96.

Cascardo, J.C.M., Almeida, R.S., Buzeli, R.A.A., Carolino, S.M.B., Otoni, W.C. and Fontes, E.P.B. (2000) The phosphorylation state and

expression of soybean BiP isoforms are differentially regulated following abiotic stresses. *J. Biol. Chem.* **275,** 14494-14500.

Cascardo, J.C.M., Buzeli, R.A.A., Almeida, R.S., Otoni, W.C. and Fontes E.P.B. (2001) Differential expression of the soybean BiP gene family. *Plant Sci.* **160,** 273-281.

Chen X, Shen J, Prywes R (2002) The luminal domain of ATF6 senses endoplasmic reticulum (ER) stress and causes translocation of ATF6 from the ER to the Golgi. *J. Biol. Chem.* **277,** 13045-13052.

Cho EK, Hong CB (2006) Over-expression of tobacco NtHSP70-1 contributes to drought-stress tolerance in plants. *Plant Cell Rep.* **25,** 349-358.

Cox, J.S., Shamu, C.E. and Walter, P. (1993) Transcriptional induction of genes encoding endoplasmic-reticulum resident proteins requires a transmembrane protein-kinase. *Cell* **73,** 1197-1206.

Cox JS, Walter P (1996) A novel mechanism for regulating activity of a transcription factor that controls the unfolded protein response. *Cell* **87,** 391-404.

Dejardin, A., Sokolov, L.N. and Kleczkowski, L.A. (1999) Sugar/osmoticum levels modulate differential abscisic acid-independent expression of two stress-responsive sucrose synthase genes in Arabidopsis. *Biochem. J.* **344,** 503-509.

Delessert, C., Kazan, K., Wilson, I.W., Van Der Straeten, D., Manners, J., Dennis, E.S. and Dolferus, R. (2005) The transcription factor ATAF2 represses the expression of pathogenesis-related genes in Arabidopsis. *Plant J.* **43,** 745-757.

Denecke, J., Carlsson, L.E., Vidal, S., Hoglund, A.S., Ek, B., van Zeijl, M.J., Sinjorgo, K.M.C. and Palva E.T. (1995) The tobacco homolog of mammalian calreticulin is present in protein complexes in vivo**.** *Plant Cell* **7,** 391-406.

Denekamp, M. and Smeekens, S.C. (2003) Integration of wounding and osmotic stress signals determines the expression of the AtMYB102 transcription factor gene. *Plant Physiol.* **132,** 1415-1423.

Dixon, D.P., Cummins, I., Cole, D.J. and Edwards, R. (1998) Glutathione-mediated detoxification systems in plants. *Curr. Opin. Plant Biol*. **1,** 258-266.

Dong, J.G., Fernandezmaculet, J.C. and Yang, S.F. (1992) Purification and characterization of 1-aminocyclopropane-1-carboxylate oxidase from apple fruit. *Proc. Natl. Acad. Sci*. **89,** 9789-9793.

Dorner AJ, Wasley LC, Kaufman RJ (1992) Overexpression Of Grp78 Mitigates Stress Induction Of Glucose Regulated Proteins And Blocks Secretion Of Selective Proteins In Chinese-Hamster Ovary Cells. *Embo J.* **11,** 1563-1571.

Dorner, A.J., Wasley, L.C., Raney, P., Haugejorden, S., Green, M. and Kaufman, R.J. (1990) The stress response in chinese-hamster ovary cells - Regulation of Erp72 and protein disulfide isomerase expression and secretion. *J. Biol. Chem.* **265,** 22029-22034.

Duval, M., Hsieh, T., Kim, S. and Thomas, T. (2002) Molecular characterization of AtNAM: a member of the Arabidopsis NAC domain superfamily. *Plant Mol. Biol.* **50,** 237-248.

Edwards, R., Dixon, D.P. and Walbot, V. (2000) Plant glutathione S-transferases: enzymes with multiple functions in sickness and in health. *Trends Plant. Sci*. **5,** 193-198.

Ellgaard L, Helenius A (2003) Quality control in the endoplasmic reticulum. *Nat. Rev. Mol. Cell Biol.* **4,** 181-191.

Ellgaard L, Molinari M, Helenius A (1999) Setting the standards: Quality control in the secretory pathway. *Science* **286,** 1882-1888.

Feder ME, Hofmann GE (1999) HEAT-SHOCK PROTEINS, MOLECULAR CHAPERONES, AND THE STRESS RESPONSE: Evolutionary and Ecological Physiology. *Annu. Rev. Physiol.* **61,** 243-282.

Fewell SW, Travers KJ, Weissman JS, Brodsky JL (2001) The action of molecular chaperones in the early secretory pathway. *Annu. Rev. Genet.* **35,** 149-191.

Fowler, S. and Thomashow, M.F. (2002) Arabidopsis transcriptome profiling indicates that multiple regulatory pathways are activated during cold acclimation in addition to the CBF cold response pathway. *Plant Cell* **14,** 1675-1690.

Frand AR, Kaiser CA (1998) The ERO1 gene of yeast is required for oxidation of protein dithiols in the endoplasmic reticulum. *Mol. Cell* **1,** 161-170.

Fujita, M., Fujita, Y., Maruyama, K., Seki, M., Hiratsu, K., Ohme-Takagi, M., Tran, L.S.P., Yamaguchi-Shinozaki, K. and Shinozaki, K. (2004) A dehydration-induced NAC protein, RD26, is involved in a novel ABA-dependent stress-signaling pathway. *Plant J.* **39,** 863-876.

Gerber J, Muhlenhoff U, Hofhaus G, Lill R, Lisowsky T (2001) Yeast Erv2p is the first microsomal FAD-linked sulfhydryl oxidase of the Erv1p/Alrp protein family. *J. Biol. Chem.* **276,** 23486-23491.

Gething, M.J. (1999) Role and regulation of the ER chaperone BiP. Semin. *Cell Dev. Biol.* **10,** 465-472.

Guo, Y., Cai, Z. and Gan, S. (2004) Transcriptome of Arabidopsis leaf senescence. *Plant Cell Environ*. **27,** 521-549.

Gupta, A., Heinen, J., Holaday, A., Burke, J. and Allen, R. (1993) Increased resistance to oxidative stress in transgenic plants that overexpress chloroplastic Cu/Zn superoxide-dismutase. *Proc. Natl. Acad. Sci.* **90,** 1629-1633.

Haas IG, Wabl M (1983) Immunoglobulin Heavy-Chain Binding-Protein. *Nature* **306,** 387-389.

Hamman, B.D., Hendershot, L.M. and Johnson, A.E. (1998) BiP maintains the permeability barrier of the ER membrane by sealing the lumenal end of the translocon pore before and early in translocation. *Cell* **92,** 747-758.

Harding, H.P., Zhang, Y.H., Bertolotti, A., Zeng, H.Q. and Ron, D. (2000) Perk is essential for translational regulation and cell survival during the unfolded protein response. *Mol. Cell* **5,** 897-904.

Harding, H.P., Zhang, Y.H. and Ron, D. (1999) Protein translation and folding are coupled by an endoplasmic-reticulum-resident kinase. *Nature* **397,** 271-274.

Harding, H.P., Zhang, Y.H., Zeng, H.Q., Novoa, I., Lu, P.D., Calfon, M., Sadri, N., Yun, C., Popko, B., Paules, R., Stojdl, D.F., Bell, J.C.,

Hettmann, T., Leiden, J.M. and Ron, D. (2003) An integrated stress response regulates amino acid metabolism and resistance to oxidative stress. *Mol. Cell* **11,** 619-633.

Haze, K., Yoshida, H., Yanagi, H., Yura, T. and Mori, K. (1999) Mammalian transcription factor ATF6 is synthesized as a transmembrane protein and activated by proteolysis in response to endoplasmic reticulum stress. *Mol. Biol. Cell* **10,** 3787-3799.

Hegde, P., Qi, R., Abernathy, K., Gay, C., Dharap, S., Gaspard, R., Hughes, J.E., Snesrud, E., Lee, N. and Quackenbush, J. (2000) A concise guide to cDNA microarray analysis. *Biotechniques* **29,** 548-562.

Hollien J, Weissman JS (2006) Decay of endoplasmic reticulum-localized mRNAs during the unfolded protein response. *Science* **313,** 104-107.

Holmberg, N. and Bulow, L. (1998) Improving stress tolerance in plants by gene transfer. *Trends Plant. Sci.* **3,** 61-66.

Houston, N.L., Fan, C.Z., Xiang, Q.Y., Schulze, J.M., Jung, R. and Boston, R.S. (2005) Phylogenetic analyses identify 10 classes of the protein disulfide isomerase family in plants, including single-domain protein disulfide isomerase-related proteins. *Plant Physiol.* **137,** 762-778.

Hsieh, T., Lee, J., Charng, Y. and Chan, M. (2002) Tomato plants ectopically expressing Arabidopsis CBF1 show enhanced resistance to water deficit stress. *Plant Physiol.* **130,** 618-626.

Hu, C.A.A., Delauney, A.J. and Verma, D.P.S. (1992) A bifunctional enzyme (Delta-1-Pyrroline-5-Carboxylate Synthetase) catalyzes the

1st 2 steps in proline biosynthesis in plants. *Proc. Natl. Acad. Sci*. **89,** 9354-9358.

Hu, H., Dai, M., Yao, J., Xiao, B., Li, X., Zhang, Q. and Xiong, L. (2006) Overexpressing a NAM, ATAF, and CUC (NAC) transcription factor enhances drought resistance and salt tolerance in rice. *Proc. Natl. Acad. Sci*. **103,** 12987-12992.

Hubbard SC, Ivatt RJ (1981) Synthesis And Processing Of Asparagine-Linked Oligosaccharides. *Annu. Rev. Biochem.* **50,** 555-583.

Jaglo-Ottosen, K., Gilmour, S., Zarka, D., Schabenberger, O. and Thomashow, M. (1998) *Arabidopsis* CBF1 overexpression induces COR genes and enhances freezing tolerance. *Science* **280,** 104-106.

Jia, J.P., Fu, J..J, Zheng, J., Zhou, X., Huai, J.L., Wang, J.H., Wang, M., Zhang, Y., Chen, X.P., Zhang, J.P., Zhao, J.F., Su. Z., Lv, Y.P. and Wang, G.Y. (2006) Annotation and expression profile analysis of 2073 full-length cDNAs from stress-induced maize (Zea mays L.) seedlings. *Plant J.* **48,** 710-727.

John, I., Hackett, R., Cooper, W., Drake, R., Farrell, A. and Grierson, D. (1997) Cloning and characterization of tomato leaf senescence-related cDNAs. *Plant Mol. Biol.* **33,** 641-651.

Kamauchi, S., Nakatani, H., Nakano, C. and Urade, R. (2005) Gene expression in response to endoplasmic reticulum stress in Arabidopsis thaliana. *Febs J.* **272,** 3461-3476.

Kasuga, M., Liu, Q., Miura, S., Yamaguchi-Shinozaki, K. and Shinozaki, K. (1999) Improving plant drought, salt, and freezing tolerance by

gene transfer of a single stress-inducible transcription factor. *Nat Biotechnol*. **17,** 287-291.

Kimata, Y., Kimata, Y.L., Shimizu, Y., Abe, H., Farcasanu, R.C., Takeuchi, M., Rose, M.D. and Kohno, K. (2003) Genetic evidence for a role of BiP/Kar2 that regulates Ire1 in response to accumulation of unfolded proteins. *Mol. Biol. Cell* **14,** 2559-2569.

Kimata, Y., Oikawa, D., Shimizu, Y., Ishiwata-Kimata, Y. and Kohno, K. (2004) A role for BiP as an adjustor for the endoplasmic reticulum stress-sensing protein Ire 1. *J. Cell Biol.* **167,** 445-456.

Kirst, M.E., Meyer, D.J., Gibbon, B.C., Jung, R. and Boston, R.S. (2005) Identification and characterization of endoplasmic reticulum-associated degradation proteins differentially affected by endoplasmic reticulum stress. *Plant Physiol.* **138,** 218-231.

Kleizen, B. and Braakman, I. (2004) Protein folding and quality control in the endoplasmic reticulum. *Curr. Opin. Cell Biol*. **16,** 343-349.

Koizumi, N., Martinez, I.M., Kimata, Y., Kohno, K., Sano, H. and Chrispeels, M.J. (2001) Molecular characterization of two arabidopsis Ire1 homologs, endoplasmic reticulum-located transmembrane protein kinases. *Plant Physiol*. **127,** 949-962.

Kornfeld R, Kornfeld S (1985) Assembly Of Asparagine-Linked Oligosaccharides. *Annu. Rev. Biochem.* **54,** 631-664.

Kozutsumi Y, Segal M, Normington K, Gething MJ, Sambrook J (1988) The Presence Of Malfolded Proteins In The Endoplasmic-Reticulum Signals The Induction Of Glucose-Regulated Proteins. *Nature* **332,** 462-464.

Kreps, J.A., Wu, Y.J., Chang, H.S., Zhu, T., Wang, X. and Harper, J.F. (2002) Transcriptome changes for Arabidopsis in response to salt, osmotic, and cold stress. *Plant Physiol.* **130,** 2129-2141.

Leborgne-Castel, N., Jelitto-Van Dooren, E., Crofts, A.J. and Denecke, J. (1999) Overexpression of BiP in tobacco alleviates endoplasmic reticulum stress. *Plant Cell* **11,** 459-469.

LeClere, S., Tellez, R., Rampey, R.A., Matsuda, S.P.T. and Bartel, B. 2002) Characterization of a family of IAA-amino acid conjugate hydrolases from Arabidopsis. *J. Biol. Chem*. **277,** 20446-20452.

Lievremont, J.P., Rizzuto, R., Hendershot, L. and Meldolesi, J. (1997) BiP, a major chaperone protein of the endoplasmic reticulum lumen, plays a direct and important role in the storage of the rapidly exchanging pool of Ca2+. *J. Biol. Chem.* **272,** 30873-30879.

Lin, J.F. and Wu, S.H. (2004) Molecular events in senescing Arabidopsis leaves. *Plant J.* **39,** 612-628.

Liu CY, Wong HN, Schauerte JA, Kaufman RJ (2002) The protein kinase/endoribonuclease IRE1 alpha that signals the unfolded protein response has a luminal N-terminal ligand-independent dimerization domain. *J. Biol. Chem.* **277,** 18346-18356.

Ludwig, A.A. and Tenhaken, R. (2001) A new cell wall located n-rich protein is strongly induced during the hypersensitive response in Glycine max L. *Eur. J. Plant Pathol.* **107,** 323-336.

Ma, Y.J. and Hendershot, L.M. (2004) ER chaperone functions during normal and stress conditions. *J. Chem. Neuroanat*. **28,** 51-65.

MacMillan, J. (1997) Biosynthesis of the gibberellin plant hormones. *Nat. Prod. Rep.* **14,** 221-243.

Mahajan, S. and Tuteja, N. (2005) Cold, salinity and drought stresses: An overview. *Arch. Biochem. Biophys*. **444,** 139-158.

Martinez, I.M. and Chrispeels, M.J. (2003) Genomic analysis of the unfolded protein response in Arabidopsis shows its connection to important cellular processes. *Plant Cell* **15,** 561-576.

Mittler, R. and Zilinskas, B.A. (1994) Regulation of pea cytosolic ascorbate peroxidase and other antioxidant enzymes during the progression of drought stress and following recovery from drought. *Plant J.* **5,** 397-405.

Molinari M, Calanca V, Galli C, Lucca P, Paganetti P (2003) Role of EDEM in the release of misfolded glycoproteins from the calnexin cycle. *Science* **299,** 1397-1400.

Molinari, M., Galli, C., Piccaluga, V., Pieren, M. and Paganetti, P. (2002) Sequential assistance of molecular chaperones and transient formation of covalent complexes during protein degradation from the ER. *J. Cell Biol*. **158,** 247-257.

Mori, K., Ma, W.Z., Gething, M.J. and Sambrook, J. (1993) A Transmembrane protein with a Cdc2+/Cdc28-related kinase-activity is required for signaling from the ER to the nucleus. *Cell* **74,** 743-756.

Morris JA, Dorner AJ, Edwards CA, Hendershot LM, Kaufman RJ (1997) Immunoglobulin binding protein (BiP) function is required to protect cells from endoplasmic reticulum stress but is not required for the secretion of selective proteins. *J. Biol. Chem.* **272,** 4327-4334.

Muller, J., Piffanelli, P., Devoto, A., Miklis, M., Elliott, C., Ortmann, B., Schulze-Lefert, P. and Panstruga, R. (2005) Conserved ERAD-Like quality control of a plant polytopic membrane protein. *Plant Cell* **17,** 149-163.

Nishikawa, S., Fewell, S.W., Kato, Y., Brodsky, J.L. and Endo, T. (2001) Molecular chaperones in the yeast endoplasmic reticulum maintain the solubility of proteins for retrotranslocation and degradation. *J. Cell Biol.* **153,** 1061-1069.

Oda Y, Hosokawa N, Wada I, Nagata K (2003) EDEM as an acceptor of terminally misfolded glycoproteins released from calnexin. *Science* **299,** 1394-1397.

Okamura, K., Kimata, Y., Higashio, H., Tsuru, A. and Kohno, K. (2000) Dissociation of Kar2p/BiP from an ER sensory molecule, Ire1p, triggers the unfolded protein response in yeast. *Biochem. Biophys. Res. Commun*. **279,** 445-450.

Olsen, A.N., Ernst, H.A., Lo Leggio, L. and Skriver, K. (2005) NAC transcription factors: structurally distinct, functionally diverse. *Trends Plant. Sci.* **10,** 79-87.

Pilon M, Romisch K, Quach D, Schekman R (1998) Sec61p serves multiple roles in secretory precursor binding and translocation into the endoplasmic reticulum membrane. *Mol. Biol. Cell* **9,** 3455-3473.

Pollard MG, Travers KJ, Weissman JS (1998) Ero1p: A novel and ubiquitous protein with an essential role in oxidative protein folding in the endoplasmic reticulum. *Mol. Cell* **1,** 171-182.

Rao, R.V. and Bredesen, D.E. (2004) Misfolded proteins, endoplasmic reticulum stress and neurodegeneration. *Curr. Opin. Cell Biol.* **16,** 653-662.

Reymond, P., Weber, H., Damond, M. and Farmer, E.E. (2000) Differential gene expression in response to mechanical wounding and insect feeding in Arabidopsis. *Plant Cell* **12,** 707–719.

Riechmann, J.L., Heard, J., Martin, G., Reuber, L., Jiang, C.Z., Keddie, J., Adam, L., Pineda, O., Ratcliffe, O.J., Samaha, R.R., Creelman, R., Pilgrim, M., Broun, P., Zhang, J.Z., Ghandehari, D., Sherman, B.K. and Yu, C.L. (2000) Arabidopsis transcription factors: Genome-wide comparative analysis among eukaryotes. *Science* **290,** 2105-2110.

Rodrigues, S.M., Andrade, M.O., Gomes, A.P.S., DaMatta, F.M., Baracat-Pereira, M.C. and Fontes, E.P.B. (2006) Arabidopsis and tobacco plants ectopically expressing the soybean antiquitin-like ALDH7 gene display enhanced tolerance to drought, salinity, and oxidative stress. *J. Exp. Bot*. **57,** 1909-1918.

Sanders, S.L., Whitfield, K.M., Vogel, J.P., Rose, M.D. and Schekman, R.W. (1992) Sec61p and BiP directly facilitate polypeptide translocation into the ER. *Cell* **69,** 353-365.

Seki, M., Narusaka, M., Ishida, J., Nanjo, T., Fujita, M., Oono, Y., Kamiya, A., Nakajima, M., Enju, A., Sakurai, T., Satou, M., Akiyama, K., Taji, T., Yamaguchi-Shinozaki, K., Carninci, P., Kawai, J., Hayashizaki, Y. and Shinozaki, K. (2002) Monitoring the expression profiles of 7000 Arabidopsis genes under drought, cold and high-

salinity stresses using a full-length cDNA microarray. *Plant J.* **31,** 279-292.

Sevier CS, Cuozzo JW, Vala A, Aslund F, Kaiser CA (2001) A flavoprotein oxidase defines a new endoplasmic reticulum pathway for biosynthetic disulphide bond formation. *Nat. Cell Biol.* **3,** 874-882.

Sgherri, C.L.M., Pinzino, C. and Navariizzo, F. (1993) Chemical-changes and O2(-) production in thylakoid membranes under water-stress. *Physiol. Plant*. **87,** 211-216.

Shen, J.S., Chen, X., Hendershot, L. and Prywes, R. (2002) ER stress regulation of ATF6 localization by dissociation of BiP/GRP78 binding and unmasking of golgi localization signals. *Dev. Cell* **3,** 99-111.

Tenhaken, R., Doerks, T. and Bork, P. (2005) DCD - a novel plant specific domain in proteins involved in development and programmed cell death. BMC *Bioinformatics* **6,** 169.

Thibaud-Nissen, F.O., Shealy, R.T., Khanna, A. and Vodkin, L.O. (2003) Clustering of microarray data reveals transcript patterns associated with somatic embryogenesis in soybean. *Plant Physiol*. **132,** 118-136.

Torres-Schumann, S., Godoy, J.A. and Pintor-Toro, J.A. (1992) A probable lipid transfer protein gene is induced by Nacl in stems of tomato plants. *Plant Mol. Biol.* **18,** 749-757.

Tran, L.S.P., Nakashima, K., Sakuma, Y., Simpson, S.D., Fujita, Y., Maruyama, K., Fujita, M., Seki, M., Shinozaki, K. and Yamaguchi-Shinozaki, K. (2004) Isolation and functional analysis of Arabidopsis stress-inducible NAC transcription factors that bind to a drought-

responsive cis-element in the early responsive to dehydration stress 1 promoter. *Plant Cell* **16,** 2481-2498.

Travers KJ, Patil CK, Wodicka L, Lockhart DJ, Weissman JS, Walter P (2000) Functional and genomic analyses reveal an essential coordination between the unfolded protein response and ER-associated degradation. *Cell* **101,** 249-258.

Tu BP, Ho-Schleyer SC, Travers KJ, Weissman JS (2000) Biochemical basis of oxidative protein folding in the endoplasmic reticulum. *Science* **290,** 1571-1574.

Tu BP, Weissman JS (2002) The FAD- and O-2-dependent reaction cycle of Ero1-mediated oxidative protein folding in the endoplasmic reticulum. *Mol. Cell* **10,** 983-994.

Tu BP, Weissman JS (2004) Oxidative protein folding in eukaryotes: mechanisms and consequences. *J. Cell Biol.* **164,** 341-346.

Uauy, C., Distelfeld, A., Fahima, T., Blechl, A. and Dubcovsky, J. (2006) A NAC gene regulating senescence improves grain protein, zinc, and iron content in wheat. *Science* **314,** 1298-1301.

Wang, X.Z., Harding, H.P., Zhang, Y.H., Jolicoeur, E.M., Kuroda, M. and Ron, D. (1998) Cloning of mammalian Ire1 reveals diversity in the ER stress responses. *EMBO J*. **17,** 5708-5717.

Wehmeyer, N. and Vierling, E. (2000) The expression of small heat shock proteins in seeds responds to discrete developmental signals and suggests a general protective role in desiccation tolerance. *Plant Physiol.* **122,** 1099-1108.

Welihinda, A.A., Tirasophon, W., Green, S.R. and Kaufman, R.J. (1998) Protein serine/threonine phosphatase Ptc2p negatively regulates the unfolded-protein response by dephosphorylating Ire1p kinase. *Mol. Cell. Biol*. **18,** 1967-1977.

Wilkinson B, Gilbert HF (2004) Protein disulfide isomerase. *BBA-Proteins Proteomics* **1699,** 35-44.

Winkler, R.G. and Helentjaris, T. (1995) The maize Dwarf3 gene encodes a cytochrome P450-mediated early step in gibberellin biosynthesis. *Plant Cell* **7,** 1307-1317.

Xie, Q., Frugis, G., Colgan, D. and Chua, N.H. (2000) Arabidopsis NAC1 transduces auxin signal downstream of TIR1 to promote lateral root development. *Genes Dev.* **14,** 3024-3036.

Yang, Y.H., Dudoit, S., Luu, P., Lin, D.M., Peng, V., Ngai, J. and Speed, T.P. (2002) Normalization for cDNA microarray data: a robust composite method addressing single and multiple slide systematic variation. *Nucleic Acids Res*. **30**: 15.

Ye, J., Rawson, R.B., Komuro, R., Chen, X., Dave, U.P., Prywes, R., Brown, M.S. and Goldstein, J.L. (2000) ER stress induces cleavage of membrane-bound ATF6 by the same proteases that process SREBPs. *Mol. Cell* **6,** 1355-1364.

Yoshiba, Y., Kiyosue, T., Katagiri, T., Ueda, H., Mizoguchi, T., Yamaguchishinozaki, K., Wada, K., Harada, Y. and Shinozaki, K. (1995) Correlation between the induction of a gene for Delta(1)-Pyrroline-5-Carboxylate Synthetase and the accumulation of proline in *Arabidopsis-thaliana* under osmotic-stress. *Plant J.* **7,** 751-760.

Zhu, J. (2001) Plant salt tolerance. *Trends Plant. Sci*. **6,** 66-71.

Supplementary Material

Table S1. Genes analyzed by qRT-PCR and primers for soybean BiP isoforms.

Clone description	Clone acession #	Forward primer 5'-3'	Reverse primer 5'-3'
Rna helicase	AI736067	TAACCCTAGCCCCTTCGCCT	GCCTTGTCGTCTTCCTCCTCG
60S ribosomal protein L30	AW309098	AAAGTGGACCAAGGCATATCGTCG	TCAGGACATTCTCCGCAAGATTCC
histone H2A	AI795114	CTGGGAATGCAAGCAAGGATCTG	GTGAGGAATGACACCACCACCAG
calnexin	AW508066	TGATGGGGAGGAGAAGAAAAAGGC	CACTTGGGTTTGGGATCTTGGCTC
seed maturation protein	AW397921	GCCGAACTGAGGAAAAGACGAACC	CTTGGGCTGTTTGTTGGGTCTTC
PDI-like(1)	AW567827	TTGGTTGAAGGCGTACAAGGATGG	ACTCCAGCAGAACATTCTTCCCAG
PDI-like(2)	AW568784	TTTGGTGTCTGATGGAAACGGTGG	CACAGTTCTGACGCACTTTGGGTG
PDI-like(3)	AW277660	CCGAAAAGGGAGAGGAGGACTTC	TCTGGGTCACCGAAAGGCAA
ATAF2 protein	AW459852	CGCTAGGGATCAAGAAAGCTCTGG	TTGGAGGCAGATCGGTCAACATTG
NAM protein	AW459732	ACGGAGACTTCAGATTCGGTGC	CATCGTTATTCCACTTGGGGTCGC
unknown	AW186110	GTTGACGCCGAAGAGGAGATAGATGG	ACATCGGGATGAAGAAGAAGGTGTCG
N-rich(1)	AI973541	TACAGGCATCCAATTTGGCGAACC	TGACTTGAAAGAGTTGATCTCACCCC
N-rich(2)	AW184865	CAAGGCTGCTGGCGACAAGATA	CGTGGAGGCAGACCGAAGAG
ubiquitin-associated protein (UBA)	AW508375	AGTCTGGCACAAGGGAACTCAACT	GTGCTGTGAAGTCAACGGCAATGT
eukaryotic translation initiation factor 5	AW472364	TGGCTCTGATGAAGACCACACT	TTCTTGGATACGTTGACGGGCA
glutathione S-transferase(1)	AW472161	CGGTTCTCATCCACAATGGCAAAC	CAGCCCAGAATCTAGCCTGAGC
glutathione S-transferase(2)	AW397276	GGCAAACCCATTTCCGAATCCCTC	ATCAGCCCAGAATCTAGCCTGAGC
BiPA	U08384	CGAGCTCTAGAGATGTTGTTGCTT	TACGTAGACGGCTGTAGTTCC
BiPC	U08382	CGAGCGCACCTTCAACTTAACC	CAACATGGCCATTCTTGTAAACACCG
BiPD	AF031241	ATCTGGAGGAGCCCTAGGCGGTGG	CTTGAAGAAGCTTCGTCGTAAAACTAAG

Table S2. Genes up-regulated by TUN and AZC treatments, but not by PEG treatment.

	PEG mean	p-value	TUN mean	p-value	AZC mean	p-value	Clone accession #	Blast hit acession #	e-value
Class: protein folding									
Subclass: heat shock protein (HSP)									
BiP isoform D	-2.30	0.008	37.13	0.000	31.41	0.000	AW509482	AAK21920	3.E-101
BiP	-2.43	0.022	29.42	0.001	20.75	0.000	AW507892	BAD95470	5.E-68
BiP	-2.16	0.023	27.22	0.034	31.90	0.000	AW471814	BAD95470	1.E-76
BiP isoform D	-1.78	0.029	25.60	0.000	23.72	0.000	AF031241		
BiP isoform C	-1.30	0.574	20.92	0.017	8.32	0.023	U08382		
BiP isoform A	-1.16	0.467	3.16	0.050	2.04	0.005	U08384		
luminal binding protein (BiP)	-1.17	0.250	2.26	0.000	2.10	0.007	AW318038	BAA12348	4.00E-15
heat shock protein 70	1.59	0.017	2.11	0.015	14.20	0.000	AW279462	AAV98051	2.00E-50
putative heat shock protein	1.25	0.517	1.93	0.003	1.57	0.012	AI930729	AAM63342	1.00E-20
molecular chaperone Hsp90-2	1.08	0.495	1.83	0.019	12.34	0.000	AW278784	AAR12194	2.00E-82
Subclass: calnexin									
calnexin homolog precursor	-2.00	0.015	22.76	0.000	15.03	0.000	AW508066	Q39817	1.E-82
calnexin homolog precursor	-1.67	0.005	15.69	0.001	7.16	0.000	AW397007	Q39817	9.E-59
calnexin homolog precursor	-1.76	0.044	12.82	0.000	6.09	0.000	AW569128	BAD81043	9.E-78
calnexin homolog precursor	1.03	0.656	2.72	0.003	1.91	0.001	AI748042	Q39817	2.00E-51
calnexin homolog precursor	1.08	0.215	1.94	0.025	1.77	0.011	AI748065	AAA80588	2.00E-26
Subclass: protein disulfide isomerase (PDI)									
protein disulfide isomerase	1.22	0.090	9.69	0.003	4.98	0.003	AW567827	CAA77575	9.00E-94
protein disulfide isomerase	1.19	0.361	6.14	0.001	2.70	0.000	AW432994	CAA77575	3.00E-16
Class: ER-associated protein degradation									
CDC48-like protein	-1.70	0.009	10.57	0.000	5.78	0.001	AW509037	AAP53974	5.E-71
putative Der1-like protein	1.03	0.821	4.44	0.000	5.12	0.004	AW507612	XP_470428	6.00E-84
proteasome subunit alpha type 7	-1.09	0.806	3.31	0.001	1.63	0.024	AW508980	Q9SXU1	3.00E-89
polyubiquitin	1.30	0.202	1.98	0.022	7.15	0.001	AW508978	AAX40652	7.00E-116

Table S2. *(Continued from previous page.)*

	PEG mean	p-value	TUN mean	p-value	AZC mean	p-value	Clone accession #	Blast hit acession #	e-value
ubiquitin conjugating enzyme	1.08	0.405	1.65	0.034	1.53	0.001	AW597856	NP_566331	3.00E-29
Class: translation regulation									
40S ribosomal protein S26	-1.11	0.665	3.02	0.002	1.79	0.019	AW507665	AAD47346	1.00E-37
60S ribosomal protein L12	-1.15	0.248	2.77	0.010	1.75	0.006	AW185793	AAR83868	2.00E-53
40S ribosomal protein S18	-1.15	0.382	2.76	0.002	1.99	0.012	AW508776	AAG12853	2.00E-67
ribosomal protein L29	-1.00	0.967	2.63	0.007	1.81	0.000	AW507673	BAA96072	2.00E-22
60S acidic ribosomal protein	-1.22	0.205	2.62	0.002	2.49	0.007	AW568451	P50346	2.00E-65
60s ribosomal protein L21	-1.03	0.396	2.30	0.002	2.13	0.000	AW508946	AAP80636	2.00E-30
60S ribosomal protein L7	1.10	0.307	2.26	0.010	1.65	0.020	AI735809	ABB16984	2.00E-73
60S ribosomal protein L2	-1.14	0.611	2.11	0.015	1.79	0.033	AI736109	CAC20221	2.00E-104
translation elongation factor	-1.19	0.199	2.05	0.009	1.93	0.016	AI960794	AAG17901	2.00E-19
translation initiation factor	1.49	0.040	2.04	0.016	1.59	0.000	AW317679	NP_192881	9.00E-27
40s ribosomal protein S23	-1.04	0.714	1.98	0.033	1.50	0.002	AW185761	AAF26742	1.00E-76
40S ribosomal protein S21	-1.02	0.858	1.96	0.019	1.73	0.012	AW508414	AAU89141	1.00E-15
60s acidic ribosomal protein	1.12	0.250	1.95	0.021	1.85	0.004	AI748232	AAS20966	3.00E-09
40S ribosomal protein S16	-1.05	0.875	1.92	0.031	1.86	0.006	AW508884	AAF34799	2.00E-70
60S ribosomal protein L9	-1.01	0.959	1.88	0.030	1.68	0.006	AI748112	S19978	6.00E-89
ribosomal protein L14	1.10	0.175	1.76	0.015	1.55	0.002	AW508885	CAB79564	2.00E-22
ribosomal protein L28	1.08	0.411	1.65	0.008	1.55	0.002	AI940871	NP_916542	9.00E-43
40S ribosomal protein S17	-1.07	0.644	1.61	0.013	1.47	0.006	AW508753	AAR83866	6.00E-53
eukaryotic initiation factor	1.22	0.005	1.60	0.009	1.56	0.040	AI941021	AAG53615	2.00E-87
Class: others									
unknown	-1.02	0.830	6.19	0.001	3.15	0.049	AW100949		
lipoxygenase	1.38	0.153	6.16	0.000	3.56	0.002	AW508203	CAA47717	1.00E-26
glyceraldehyde 3-phosphate dehydrogenase	-1.25	0.544	4.21	0.011	5.06	0.007	AW567594	AAM92008	4.00E-60
putative UDP-galactose transporter	-1.28	0.031	3.96	0.002	2.78	0.025	AW508528	AAT40483	7.00E-59
unknown	-1.01	0.920	3.79	0.001	12.31	0.001	AW471972		
protein phosphatase 2C	-1.12	0.577	3.36	0.010	2.63	0.005	AW569267	CAA72341	1.00E-22

Table S2. *(Continued from previous page.)*

	PEG mean	p-value	TUN mean	p-value	AZC mean	p-value	Clone accession #	Blast hit acession #	e-value
unknown	1.05	0.456	3.22	0.000	2.40	0.002	AW471959		
unknown	1.39	0.109	3.18	0.011	7.74	0.001	AW186357		
unknown	1.02	0.821	2.97	0.038	4.16	0.002	AW568275		
peptidylprolyl isomerase	-1.03	0.739	2.59	0.004	1.80	0.002	AW309048	BAB10690	2.00E-54
translational inhibitor protein	-1.29	0.285	2.35	0.002	1.50	0.021	AW508686	AAM63246	1.00E-50
unknown	1.05	0.535	2.33	0.012	2.13	0.000	AW508823		
calcium ion binding protein	1.58	0.048	2.31	0.021	1.64	0.003	AW508312	NP_566657	1.00E-38
unknown	-1.01	0.877	2.29	0.005	2.58	0.006	AW508752		
unknown	1.16	0.000	2.21	0.001	2.20	0.005	AI938483		
RNA binding protein	1.06	0.423	2.21	0.002	3.79	0.020	AW507594	CAA57551	7.00E-31
protein phpsphatase 2C	1.01	0.940	2.18	0.003	1.88	0.007	AW471739	CAB90633	1.00E-38
unknown	-1.25	0.001	2.18	0.000	2.66	0.016	AW100917		
unknown	1.10	0.260	2.17	0.001	1.87	0.008	AW507857		
unknown	-1.05	0.291	2.12	0.003	2.88	0.004	AW570334		
unknown	-1.06	0.402	2.06	0.009	1.62	0.010	AW507573		
unknown	-1.33	0.202	2.01	0.002	1.94	0.002	AW471731		
unknown	1.33	0.249	1.91	0.006	2.49	0.000	AW567808		
harpin inducing protein 1-like 9	-1.02	0.890	1.91	0.011	3.14	0.017	AW432916	BAD22533	1.00E-27
2A phosphatase-associated protein	1.55	0.053	1.86	0.004	6.92	0.000	AW509424	NP_568783	2.00E-41
unknown	1.14	0.441	1.84	0.026	1.67	0.043	AW509441		
putative ABC transporter protein	1.41	0.093	1.83	0.002	2.16	0.017	AW277892	AAO63876	6.00E-64
poly(A)-binding protein	1.14	0.226	1.79	0.006	1.54	0.014	AW186100	AAK30205	6.00E-104
unknown	1.01	0.973	1.76	0.034	1.74	0.046	AW507518		
unknown	1.16	0.087	1.71	0.033	1.56	0.004	AW101722		
unknown	-1.06	0.421	1.68	0.001	1.59	0.000	AW507577		
histone H3	1.18	0.165	1.59	0.018	1.70	0.010	AW472128	AAV65112	6.00E-37
unknown	-1.06	0.747	1.58	0.018	4.20	0.002	AW471755		
farnesylated protein	1.05	0.761	1.54	0.001	7.99	0.003	AW101796	CAB61745	4.00E-08

Table S2. *(Continued from previous page.)*

	PEG mean	p-value	TUN mean	p-value	AZC mean	p-value	Clone accession #	Blast hit acession #	e-value
putative zinc-binding protein	1.12	0.526	1.53	0.014	2.18	0.005	AW508925	XP_467248	5.00E-71

Table S3. Genes down-regulated by TUN and AZC treatments, but not by PEG treatment.

	PEG mean	p-value	TUN mean	p-value	AZC mean	p-value	Clone acession #	Blast hit acession #	e-value
Class: regulatory proteins									
mRNA-binding protein	-2.08	0.071	-2.19	0.010	-3.57	0.002	AW508032	AAC49424	3.00E-47
putative ADP ATP carrier protein	-1.10	0.397	-2.18	0.039	-2.61	0.000	AW507801	BAE71236	4.00E-87
MADS box transcription factor	-1.03	0.593	-1.64	0.025	-2.13	0.008	AI959798	CAC81072	4.00E-52
serine/threonine protein kinase-like protein	-1.49	0.170	-1.58	0.003	-1.48	0.011	AW472140	BAB01040	5.00E-32
GTP-binding protein TypA	-1.54	0.000	-1.57	0.007	-1.46	0.016	AI736180	AAR17698	1.00E-32
Class: others									
beta-amylase	-1.70	0.193	-4.13	0.009	-2.00	0.035	AW509022	BAD93291	1.00E-13
aquaporin	-1.15	0.728	-3.29	0.002	-4.60	0.013	AW507966	AAV69744	3.00E-38
unknown	-1.39	0.051	-2.22	0.042	-1.55	0.019	AW508041		
caffeic acid O-methyltransferase	1.30	0.039	-2.10	0.012	-3.97	0.004	AI930875	BAC78828	1.00E-18
flavanone 3-hydroxylase	-1.17	0.197	-1.93	0.005	-2.48	0.018	AW277481	AAU06216	1.00E-108
late embryogenesis abundant protein	1.13	0.001	-1.89	0.008	-2.44	0.001	AW459847	CAC39160	1.00E-08
putative glycosyl transferase	1.03	0.777	-1.86	0.012	-2.69	0.007	AW185913	NP_191825	9.00E-49
unknown	-1.52	0.084	-1.84	0.005	-1.55	0.001	AI748057		
lipid transfer like protein	1.13	0.241	-1.81	0.012	-1.48	0.029	AI736270	CAA56113	2.00E-18
unknown	1.74	0.003	-1.77	0.049	-1.72	0.005	AW186103		
unknown	1.22	0.006	-1.72	0.014	-1.78	0.005	AW185765		
cytochrome P450-like protein	-1.20	0.226	-1.69	0.001	-2.13	0.001	AI794818	NP_174713	1.00E-36
putative glycosyl hydrolase	-1.51	0.117	-1.68	0.008	-2.22	0.014	AW507956	AAO50728	7.00E-33
SHOOT1 protein	-1.35	0.104	-1.67	0.006	-1.49	0.007	AW101186	AAK37555	4.00E-23
unknown	-1.20	0.135	-1.59	0.023	-2.02	0.015	AW567713		
unknown	-1.64	0.053	-1.53	0.021	-2.23	0.002	AW508077		
unknown	-1.53	0.101	-1.51	0.014	-1.50	0.001	AW397753		

Table S4. Genes up-regulated by PEG treatment, but not by AZC and TUN treatments.

	PEG mean	p-value	TUN mean	p-value	AZC mean	p-value	Clone acession #	Blast hit acession #	e-value
Class: cellular protectants									
Subclass: LEA-family proteins									
seed maturation protein PM30	39.24	0.029	1.18	0.306	-1.08	0.531	AW397921	AAD30864	2.00E-27
seed maturation protein PM34	6.31	0.005	-1.07	0.433	1.11	0.357	AI735868	AAF89645	6.00E-65
seed maturation protein LEA 4	5.87	0.021	1.07	0.485	1.76	0.016	AW568142	CAA45126	2.00E-74
seed maturation protein PM34	3.24	0.023	-1.21	0.033	-1.21	0.053	AW507695	AAF89645	1.00E-10
dehydrin	2.96	0.004	1.07	0.353	1.19	0.035	AI748083	AAB71225	1.00E-30
seed maturation protein PM34	2.25	0.001	1.02	0.839	-1.10	0.340	AW568206	AAF89645	6.00E-47
putative late-embryogenesis protein	2.20	0.040	1.35	0.186	1.20	0.109	AW509302	AAW31666	2.00E-27
dehydrin	1.96	0.002	1.03	0.544	1.12	0.176	AI748086	AAB71225	5.00E-27
seed maturation protein PM41	1.88	0.006	-1.21	0.025	1.11	0.104	AW397256	AAD51628	1.00E-34
putative late embryogenesis abundant protein	1.71	0.019	1.42	0.085	1.27	0.099	AW186358	XP_470376	5.00E-75
Subclass: HSP and protein folding									
PDI-like protein	4.22	0.003	1.12	0.642	-1.24	0.207	AW277660	AAM64945	2.00E-37
protein disulfide isomerase	3.35	0.007	-1.13	0.657	-1.32	0.014	AW568784	AAV50008	1.00E-22
70 kDa heat shock cognate protein	1.67	0.003	1.45	0.103	6.53	0.001	AW567735	AAS57912	3.00E-90
Subclass: osmoprotectant biosynthesis									
delta 1-pyrroline-5-carboxylate synthetase	3.48	0.003	1.04	0.816	1.16	0.031	AW309049	CAG29643	8.00E-30
sucrose synthase	3.19	0.015	1.75	0.133	1.44	0.011	AW164630	AAC28107	2.00E-94
sucrose synthase	2.87	0.010	1.17	0.436	1.05	0.410	AI973540	BAA88904	3.00E-26
Subclass: carbohydrate metabolism									
sucrose-phosphatase	1.95	0.005	-1.03	0.703	1.22	0.057	AW308920	AAG31076	1.00E-53
carbohydrate oxidase	1.90	0.002	1.08	0.666	1.04	0.389	AW317925	AAL77103	6.00E-52
glucose-6-phosphate isomerase	1.71	0.008	-1.03	0.810	-1.08	0.306	AW507818	CAB55566	2.00E-47
Subclass: sugar transport									

Table S4 *(Continued from previous page.)*

	PEG mean	PEG p-value	TUN mean	TUN p-value	AZC mean	AZC p-value	Clone accession #	Blast hit acession #	e-value
sugar transporter family protein	2.49	0.012	-1.09	0.341	-1.17	0.173	AW317898	NP_174313	2.00E-62
Subclass: detoxification									
glutathione peroxidase	5.31	0.004	1.28	0.026	1.36	0.000	AW567877	AAQ03092	4.00E-77
glutathione peroxidase	2.94	0.007	1.00	0.876	1.13	0.181	AI735901	AAQ03092	7.00E-51
Subclass: senescence									
senescence-associated protein	2.27	0.023	1.38	0.133	1.31	0.005	AI759650	BAD42919	8.00E-69
Subclass: protease inhibitor									
cysteine proteinase inhibitor	2.61	0.002	1.18	0.122	1.79	0.022	AW460045	BAA19608	3.00E-42
protease inhibitor	1.70	0.048	1.31	0.103	1.23	0.135	AI930853	AAB19651	1.00E-14
Subclass: lipid transfer proteins									
lipid transfer protein I	3.13	0.002	-3.20	0.099	-8.05	0.001	AW185914	AAQ74627	3.00E-25
lipid tranfer protein II	2.46	0.008	-1.14	0.218	-1.01	0.928	AW433055	AAQ74628	2.00E-30
Class: regulatory proteins									
NAC domain protein NAC2	4.75	0.004	1.31	0.087	2.11	0.110	AW433077	AAY46122	3.00E-32
putative Serine/threonine-protein kinase	2.77	0.030	-1.04	0.667	1.59	0.063	AW460118	NP_912073	6.00E-37
protein phosphatase-2C	2.26	0.002	1.05	0.750	1.36	0.005	AW279540	AAC36697	2.00E-72
NAC domain protein NAC3	2.18	0.007	1.27	0.067	2.00	0.007	AW457909	AAY46123	9.00E-59
bZip transcription factor	1.87	0.005	-1.06	0.659	-1.01	0.893	AI941155	BAD42432	1.00E-26
Class: others									
unknown	7.29	0.014	3.58	0.007	1.16	0.278	AI930841		
translation initiation factor 5A	5.64	0.002	1.40	0.122	1.03	0.721	AW278792	AAK55848	1.00E-78
GIR1	5.00	0.008	1.18	0.407	-1.01	0.633	AW397327	AAY51975	3.00E-37
flavin-containing monooxygenase	4.53	0.007	1.66	0.050	1.05	0.690	AW279019	NP_199202	6.00E-35
polygalacturonase-like protein	4.52	0.003	-1.02	0.857	1.11	0.074	AW508084	AAP33475	8.00E-96
cyclin	4.35	0.000	1.17	0.195	2.04	0.013	AW279562	CAA57555	1.00E-71
unknown	4.04	0.001	1.42	0.037	5.29	0.010	AW508125		
unknown	3.79	0.009	1.08	0.640	1.20	0.205	AW569110		
Malate synthase	3.69	0.001	1.02	0.859	-1.05	0.367	AW472610	AAC37465	2.00E-18

Table S4 *(Continued from previous page.)*

	PEG mean	p-value	TUN mean	p-value	AZC mean	p-value	Clone accession #	Blast hit acession #	e-value
unknown	3.43	0.008	1.11	0.177	1.04	0.674	AW508192		
calcium binding protein	3.38	0.001	1.18	0.019	1.04	0.767	AW185778	CAE51349	6.00E-53
unknown	3.35	0.000	-1.01	0.836	1.19	0.070	AW101685		
phospholipase C	3.35	0.004	-1.10	0.515	1.22	0.018	AI794656	AAQ95730	2.00E-112
putative ribosomal protein L21	3.20	0.001	-1.30	0.155	1.98	0.004	AW471733	XP_475904	2.00E-39
GIR1	3.14	0.005	-1.13	0.412	-1.12	0.427	AI748264	AAY51975	1.00E-22
putative cellulose synthase	3.06	0.001	-1.01	0.937	-1.20	0.018	AW279531	NP_921915	3.00E-91
unknown	3.05	0.009	1.09	0.413	1.40	0.013	AI930894		
epoxide hydrolase	2.99	0.004	-1.09	0.153	1.16	0.034	AW277787	CAA55294	2.00E-89
unknown	2.93	0.000	1.04	0.612	1.33	0.002	AW164308		
S-adenosylmethionine decarboxylase	2.85	0.004	-1.15	0.131	1.27	0.068	AW164411	AAM44307	4.00E-54
unknown	2.83	0.001	-1.02	0.747	1.57	0.023	AW508757		
ferritin	2.80	0.008	-1.03	0.894	-1.31	0.042	AW186337	AAB18928	4.00E-77
unknown	2.79	0.000	-3.08	0.100	-8.47	0.000	AW185926		
unknown	2.79	0.007	-2.52	0.084	-14.07	0.000	AW568531		
unknown	2.71	0.013	1.64	0.030	-1.04	0.428	AW471785		
unknown	2.68	0.009	1.30	0.026	7.11	0.001	AW508112		
putative gamma-lyase	2.48	0.017	1.32	0.008	1.23	0.016	AW279500	NP_922347	3.00E-38
formate dehydrogenase	2.44	0.004	1.43	0.023	1.10	0.125	AW460106	NP_196982	2.00E-46
malate synthase	2.38	0.022	-1.03	0.643	1.18	0.065	AW471927	AAC37465	1.00E-98
unknown	2.35	0.002	1.30	0.074	2.33	0.008	AW508080		
ion channel domain-containing protein	2.26	0.034	-1.20	0.139	6.17	0.001	AW508233	BAD28130	4.00E-48
unknown	2.23	0.013	1.01	0.876	-1.10	0.287	AW279024		
epoxide hydrolase	2.13	0.009	-1.18	0.271	1.05	0.584	AW568104	CAA55294	5.00E-89
39 kDa EF-Hand containing protein	2.11	0.002	1.18	0.215	1.02	0.623	AW185781	CAA04670	4.00E-60
putative inorganic pyrophosphatase	2.11	0.002	1.35	0.059	1.05	0.634	AI930848	NP_171613	4.00E-24
PRL1 protein	2.10	0.008	1.24	0.063	2.66	0.001	AI959838	CAA72073	6.00E-40
inositol 1,3,4-trisphosphate 5/6 kinase	2.09	0.024	1.07	0.090	-1.02	0.801	AW507587	NP_197178	2.00E-38

Table S4 *(Continued from previous page.)*

	PEG mean	p-value	TUN mean	p-value	AZC mean	p-value	Clone accession #	Blast hit acession #	e-value
aldehyde dehydrogenase	2.09	0.027	1.22	0.130	-1.20	0.175	AW508769	AAP02957	2.00E-80
peripheral-type benzodiazepine receptor	2.08	0.031	-1.08	0.392	1.04	0.382	AW568173	CAH10765	3.00E-41
unknown	2.08	0.040	1.35	0.038	1.02	0.763	AW569197		
ferritin	2.04	0.016	1.90	0.025	-1.00	0.977	AW279016	P19976	1.00E-73
epoxide hydrolase	2.03	0.006	-1.22	0.080	-1.21	0.041	AW568473	CAA55293	4.00E-90
aldehyde dehydrogenase family 7	2.02	0.013	-1.08	0.121	-1.02	0.742	AW598015	AAP02957	3.00E-60
unknown	2.01	0.019	-1.03	0.860	1.49	0.145	AW472183		
unknown	2.00	0.013	1.07	0.583	-1.32	0.042	AW568310		
Eukaryotic translation initiation factor 5	2.00	0.033	1.06	0.153	1.05	0.112	AW507641	P48724	7.00E-25
Response regulator receiver domain protein	1.97	0.003	1.52	0.092	1.06	0.477	AW278926	ABA73285	3.00E-60
unknown	1.95	0.028	1.02	0.586	1.20	0.022	AW568621		
SNF4b	1.92	0.027	-1.08	0.334	1.11	0.111	AW460050	AAO61675	3.00E-51
unknown	1.92	0.038	1.26	0.057	1.29	0.003	AI930891		
histone H3	1.90	0.030	1.47	0.006	1.70	0.072	AW460105	AAB81995	1.00E-68
unknown	1.88	0.034	1.11	0.284	1.00	0.953	AW459775		
nicotinate phosphoribosyltransferase-like protein	1.84	0.033	-1.11	0.288	-1.00	0.968	AW508812	AAP69614	3.00E-22
putative O-linked GlcNAc transferase	1.81	0.035	1.07	0.371	1.13	0.055	AW279039	AAF26789	1.00E-74
dynein light chain	1.81	0.013	1.01	0.955	1.04	0.536	AW309179	AAF29412	4.00E-36
Ca2+/H+ exchanger	1.81	0.008	-1.32	0.020	-1.35	0.060	AW459585	BAA25753	2.00E-40
Plastid-lipid associated protein	1.79	0.016	-1.02	0.934	1.05	0.500	AW509036	Q9ZWQ8	2.00E-43
serine carboxypeptidase II	1.78	0.002	1.13	0.169	1.11	0.354	AW507575	ABA93967	1.00E-65
putative amine oxidase	1.77	0.004	-1.18	0.082	-1.02	0.831	AW186466	NP_181830	2.00E-46
unknown	1.76	0.001	-1.45	0.081	-1.56	0.026	AW186144		
sulfite oxidase	1.75	0.045	1.35	0.057	2.00	0.000	AW508598	BAE48793	2.00E-43
phospholipase D	1.74	0.020	1.09	0.445	-1.27	0.021	AW567646	AAB51392	4.00E-84
unknown	1.74	0.003	-1.77	0.049	-1.72	0.005	AW186103		
ferrodoxin NADP oxidoreductase	1.73	0.028	1.62	0.002	-1.05	0.756	AW507672	CAA67796	1.00E-57

Table S4 *(Continued from previous page.)*

	PEG mean	p-value	TUN mean	p-value	AZC mean	p-value	Clone accession #	Blast hit acession #	e-value
unknown	1.73	0.050	1.20	0.297	1.70	0.005	AW568205		
unknown	1.72	0.047	4.54	0.002	1.41	0.169	AW508767		
unknown	1.71	0.000	2.72	0.004	1.22	0.010	AW186388		
beta-conglycinin alpha prime subunit	1.70	0.013	-1.09	0.289	1.03	0.810	AW317783	BAC78524	4.00E-47
unknown	1.70	0.035	-1.02	0.116	-1.07	0.434	AW308898		
alcohol-dehydrogenase	1.68	0.040	1.12	0.159	1.06	0.595	AW568339	AAC97495	7.00E-82
PRP38 pre-mRNA processing factor 38	1.68	0.016	1.24	0.001	-1.03	0.560	AW186077	XP_876900	2.00E-23
unknown	1.66	0.009	-1.00	0.980	1.02	0.625	AI748220		
synaptobrevin-like protein	1.64	0.036	1.20	0.284	1.25	0.072	AI736105	BAB08335	6.00E-67
unknown	1.64	0.006	1.04	0.614	-1.08	0.250	AW507630		

Table S5. Genes down-regulated by PEG treatment, but not by AZC and TUN treatments.

	PEG mean	p-value	TUN mean	p-value	AZC mean	p-value	Clone acession #	Blast hit acession #	e-value
Class: protein-folding proteins									
BiP	-2.43	0.022	29.42	0.001	20.75	0.000	AW507892	BAD95470	5.00E-68
BiP-isoform D	-2.30	0.008	37.13	0.000	31.41	0.000	AW509482	AAK21920	4.00E-101
BiP	-2.16	0.023	27.22	0.034	31.90	0.000	AW471814	BAD95470	1.00E-76
calnexin homolog precursor	-2.00	0.015	22.76	0.000	15.03	0.000	AW508066	Q39817	1.00E-82
putative chaperonin containing TCP1	-1.81	0.049	1.44	0.007	1.01	0.888	AW507810	XP_464810	2.00E-43
BiPD	-1.78	0.029	25.60	0.000	23.72	0.000	AF031241		
calnexin homolog precursor	-1.76	0.044	12.82	0.000	6.09	0.000	AW569128	Q39817	9.00E-78
calnexin homolog precursor	-1.67	0.005	15.69	0.001	7.16	0.000	AW397007	Q39817	9.00E-59
Class: ER-associated protein degradation									
AAA family ATPase CDC48	-1.70	0.009	10.57	0.000	5.78	0.001	AW509037	AAP53974	5.00E-71
Class: others									
unknown	-7.46	0.001	-2.49	0.058	-9.84	0.000	AW570496		
unknown	-4.09	0.034	-4.14	0.018	-1.55	0.066	AW472276		
glyceraldehyde-3-phosphate dehydrogenase	-3.86	0.007	undet.	undet.	-18.61	0.000	AW567734	ABA86963	1.00E-88
unknown	-3.50	0.005	-1.15	0.204	1.20	0.029	AW396842		
putative serine decarboxylase	-3.29	0.002	-1.02	0.890	1.15	0.096	AI938461	BAD28221	2.00E-51
putative beta-glucosidase	-3.21	0.015	-1.53	0.027	-1.05	0.661	AW459699	BAC42451	3.00E-52
chalcone reductase homologue	-3.20	0.023	-4.68	0.006	-2.87	0.066	AI938437	CAA88591	3.00E-32
unknown	-3.13	0.002	-1.28	0.074	-1.07	0.112	AW101023		
putative nitrate transporter NRT1-3	-3.10	0.002	-1.58	0.074	1.06	0.509	AW278825	BAB19758	2.00E-26
unknown	-3.08	0.003	-1.35	0.066	-1.89	0.001	AI941038		
homeodomain-leucine zipper protein 56	-2.99	0.006	-2.26	0.068	-3.59	0.001	AW508928	AAF01764	7.00E-27
unknown	-2.90	0.020	-1.20	0.173	1.00	0.984	AW508802		
photosystem II reaction center Z protein	-2.88	0.003	-2.04	0.106	-2.76	0.009	AW277587	ABC25118	8.00E-16
fiber protein Fb34	-2.86	0.003	-1.58	0.105	-1.34	0.008	AW570343	AAR07596	2.00E-55

Table S5 *(Continued from previous page.)*

	PEG mean	p-value	TUN mean	p-value	AZC mean	p-value	Clone accession #	Blast hit acession #	e-value
unknown	-2.84	0.012	4.06	0.007	-1.05	0.778	AW457905		
aldehyde oxidase	-2.82	0.001	-2.91	0.099	-7.57	0.001	AW309206	BAE72098	7.00E-67
unknown	-2.77	0.036	1.53	0.147	1.31	0.103	AW568657		
putative nitrate transporter NRT1-3	-2.74	0.013	-1.43	0.054	-1.28	0.086	AI960849	BAB19758	7.00E-24
phosphoethanolamine N-methyltransferase	-2.73	0.039	-1.49	0.024	-1.01	0.811	AW509345	AAF61950	4.00E-12
glucose-6-phosphate/phosphate-translocator precursor	-2.70	0.024	-1.53	0.267	-3.46	0.001	AW507609	AAC08525	3.00E-84
unknown	-2.67	0.001	-1.76	0.167	-1.25	0.054	AW185758		
photosystem II 23kDa polypeptide	-2.53	0.001	-1.45	0.216	-1.51	0.000	AW100965	CAA39039	1.00E-68
unknown	-2.48	0.001	-2.51	0.045	-1.80	0.054	AW100977		
chloroplast oxygen-evolving enhancer protein	-2.46	0.007	-1.03	0.146	-1.21	0.009	AW397159	AAV74404	7.00E-57
unknown	-2.46	0.011	-1.41	0.093	-1.28	0.032	AW508829		
photosystem II 5 kDa protein	-2.42	0.001	-2.24	0.054	-1.83	0.001	AW397297	CAA38027	5.00E-14
photosystem II protein	-2.32	0.002	-1.68	0.057	-1.70	0.002	AW397279	AAM61462	3.00E-09
unknown	-2.32	0.026	-1.99	0.012	-1.10	0.065	AW471607		
HMG-1 like protein	-2.28	0.001	-1.19	0.047	-2.28	0.004	AW508548	CAA41200	3.00E-45
unknown	-2.24	0.001	-1.11	0.067	-1.14	0.008	AW570215		
unknown	-2.22	0.018	-1.10	0.247	1.09	0.381	AW277700		
magnesium chelatase subunit	-2.18	0.006	-1.66	0.005	-1.31	0.158	AW101583	CAA04526	3.00E-22
granule-bound starch synthase Ib precursor	-2.18	0.007	-1.51	0.063	-1.78	0.005	AI940891	BAC76613	2.00E-39
putative uracil phosphoribosyl transferase	-2.18	0.026	-1.92	0.007	-1.40	0.051	AW278938	AAM63338	1.00E-25
unknown	-2.15	0.037	-1.67	0.099	-2.04	0.024	AW472367		
pseudo-response regulator protein	-2.14	0.003	undet.	undet.	-1.82	0.020	AW567584	AAQ83694	7.00E-27
hydroxymethyltransferase	-2.08	0.037	-1.27	0.358	-2.64	0.002	AW472022	CAB10172	1.00E-83
unknown	-2.06	0.000	-1.41	0.116	-1.51	0.004	AW186513		
unknown	-2.06	0.000	-1.04	0.448	-1.24	0.024	AW567774		
putative thiamin biosynthesis protein	-2.04	0.002	-1.61	0.074	-1.15	0.090	AW508746	AAM91156	1.00E-52
beta-tubulin	-2.03	0.023	-1.10	0.546	1.08	0.301	AW472478	CAA42777	1.00E-88

Table S5 *(Continued from previous page.)*

	PEG mean	p-value	TUN mean	p-value	AZC mean	p-value	Clone accession #	Blast hit acession #	e-value
5-adenylylsulfate reductase	-2.02	0.007	-1.10	0.438	1.18	0.223	AW508411	AAL66290	9.00E-115
unknown	-1.99	0.016	-1.03	0.807	-1.16	0.216	AW279043		
unknown	-1.98	0.006	-1.63	0.010	-1.43	0.004	AW508612		
omega-3 fatty acid desaturase	-1.97	0.006	-1.45	0.073	-1.28	0.041	AI960984	P48619	7.00E-103
putative acid phosphatase	-1.96	0.024	-1.41	0.058	-1.72	0.006	AI748106	CAE85073	2.00E-66
cytosolic glutamine synthetase	-1.94	0.011	3.95	0.001	-1.36	0.081	AW277673	AAG24873	7.00E-92
NADPH-protochlorophyllide oxidoreductase	-1.91	0.000	-1.68	0.060	-1.28	0.140	AW568896	AAD20020	1.00E-52
zinc finger (B-box type) family protein	-1.90	0.007	-1.65	0.007	-1.35	0.023	AW308945	AAK01658	2.00E-51
T complex protein	-1.90	0.012	-1.49	0.036	-1.18	0.051	AW459898	BAD53747	2.00E-73
unknown	-1.90	0.031	-1.18	0.157	-1.19	0.270	AI959820		
photosystem I subunit O	-1.90	0.032	-1.67	0.000	-1.30	0.039	AW568055	CAD37939	1.00E-46
senescence-associated protein	-1.85	0.024	-2.33	0.066	-1.10	0.124	AW471585	AAZ23261	7.00E-29
unknown	-1.84	0.002	-1.63	0.092	-1.18	0.148	AW186409		
prenyl-dependent CAAX protease	-1.83	0.007	-1.25	0.061	-1.29	0.001	AW570389	NP_568928	4.00E-21
unknown	-1.82	0.030	-1.47	0.021	-1.06	0.178	AW101826		
NADPH oxidase	-1.81	0.006	-1.43	0.125	1.13	0.193	AW309202	AAM45050	2.00E-54
acylaminoacyl-peptidase	-1.81	0.005	-1.31	0.057	-1.25	0.053	AW277632	JC8016	3.00E-20
photosystem II 5 kDa protein	-1.81	0.003	-1.27	0.054	-1.33	0.005	AW277732	CAA38027	1.00E-13
unknown	-1.79	0.003	-1.38	0.129	-1.33	0.003	AI748724		
ferredoxin-thioredoxin reductase	-1.79	0.002	1.46	0.109	-1.30	0.129	AW508189	NP_197735	2.00E-19
unknown	-1.78	0.043	-1.19	0.372	-1.06	0.370	AI941024		
unknown	-1.78	0.015	-1.61	0.003	-1.21	0.107	AI930801		
alpha-glucan phosphorylase	-1.78	0.011	-1.02	0.759	-1.10	0.234	AW185944	CAA84494	2.00E-58
ribosomal protein S2	-1.78	0.004	-1.30	0.166	-1.70	0.028	AW277768	BAB33197	3.00E-83
omega-6 fatty acid desaturase	-1.78	0.015	1.05	0.546	-1.81	0.001	AW100780	P48631	1.00E-124
unknown	-1.77	0.040	-1.04	0.636	-1.07	0.206	AW570416		
N-acetyltransferase	-1.77	0.029	-1.40	0.006	-1.32	0.019	AW507872	NP_181433	3.00E-44
unknown	-1.75	0.015	-1.26	0.143	-1.60	0.003	AI941191		

Table S5 *(Continued from previous page.)*

	PEG mean	p-value	TUN mean	p-value	AZC mean	p-value	Clone accession #	Blast hit acession #	e-value
light regulated protein	-1.75	0.008	-1.60	0.052	-1.27	0.129	AW164606	AAM65631	3.00E-23
serine/threonine Kinase	-1.73	0.001	-1.08	0.579	-1.36	0.017	AW472439	AAL23677	7.00E-14
unknown	-1.73	0.031	-1.18	0.144	-1.45	0.008	AW472415		
ribosomal protein L27	-1.73	0.048	1.06	0.408	-1.18	0.053	AW508272	AAA86950	2.00E-59
metal ion binding protein	-1.73	0.026	-1.08	0.480	-1.53	0.072	AW102551	NP_195958	7.00E-19
putative sulfolipid synthase	-1.72	0.000	-1.33	0.064	-3.44	0.002	AW186158	XP_476339	2.00E-46
unknown	-1.71	0.027	-1.15	0.440	-1.53	0.142	AI930941		
unknown	-1.70	0.017	-1.49	0.093	-1.22	0.031	AW570264		
unknown	-1.69	0.009	-1.39	0.017	-1.79	0.011	AW277490		
unknown	-1.68	0.022	1.29	0.244	-1.19	0.173	AW508126		
unknown	-1.68	0.002	-1.08	0.506	-1.08	0.595	AW277889		
unknown	-1.68	0.000	-1.40	0.096	-1.19	0.104	AI748741		
adenine phosphoribosyltransferase	-1.67	0.031	-1.09	0.529	-1.02	0.884	AW277930	NP_196677	2.00E-51
fasciclin-like arabinogalactan protein FLA2	-1.67	0.009	-1.84	0.182	-2.90	0.005	AW186452	BAE71278	5.00E-28
unknown	-1.67	0.027	-1.17	0.291	-1.05	0.463	AI748636		
oxygen-evolving enhancer protein	-1.64	0.027	-1.13	0.008	-1.20	0.073	AW509221	P14226	2.00E-88
putative UDP-rhamnose:rhamnosyltransferase	-1.64	0.010	-1.70	0.023	-1.33	0.035	AW309228	AAU09445	6.00E-21
adenosylhomocysteinase	-1.63	0.006	1.17	0.176	-1.43	0.009	AW278986	AAO89237	3.00E-86
unknown	-1.63	0.009	-1.29	0.076	-1.49	0.001	AW507811		
unknown	-1.63	0.002	1.01	0.893	-1.12	0.141	AW457954		

Table S6. Genes up-regulated by TUN, AZC and PEG treatments.

	PEG mean	p-value	TUN mean	p-value	AZC mean	p-value	Clone acession #	Blast hit acession #	e-value
Class: NAC-family members									
putative ATAF2 protein	3.93	0.002	4.33	0.031	7.19	0.002	AW459852	BAC43493	8.E-31
NAM protein	2.81	0.008	3.31	0.019	5.27	0.001	AW459732	ABE79286	1.E-33
Class: DCD-domain proteins									
N-rich protein	2.76	0.005	3.39	0.009	4.33	0.012	AI973541	CAI44933	4.E-07
N-rich protein	1.93	0.008	2.14	0.012	2.42	0.003	AW184865	CAI44933	2.E-76
Class: redox regulation									
glutathione S-transferase	3.83	0.003	3.19	0.002	2.75	0.002	AW472161	AAC18566	2.E-46
glutathione S-transferase	2.22	0.002	2.28	0.000	1.48	0.009	AW397276	AAG34800	1.E-48
Class: others									
eukaryotic translation initiation factor 5	3.56	0.002	1.54	0.028	1.84	0.015	AW472364	P48724	2.E-65
putative ubiquitin-associated (UBA) protein	3.05	0.000	3.12	0.024	2.59	0.014	AW508375	XP_466502	4.E-38
unknown	2.58	0.005	3.17	0.003	9.56	0.000	AW186110		
unknown	1.74	0.001	3.08	0.006	19.56	0.000	AW508115		

Table S7. Genes down-regulated by TUN, AZC and PEG treatments.

	PEG mean	p-value	TUN mean	p-value	AZC mean	p-value	Clone acession #	Blast hit acession #	e-value
Class: photosynthesis									
chlorophyll a/b-binding protein	-28.79	0.002	-10.26	0.028	-31.02	0.000	AW472492	AAA50172	1.E-64
LHCII type III chlorophyll a/b binding protein	-15.20	0.001	-10.48	0.004	-38.20	0.000	AW397809	AAD27877	9.E-85
putative chlorophyll a/b-binding protein	-11.01	0.004	-6.02	0.004	-8.13	0.000	AW568620	XP_482572	2.E-73
chlorophyll a/b-binding protein CP24	-9.95	0.005	-6.83	0.004	-16.75	0.000	AW568341	AAD27882	2.E-75
photosystem I chlorophyll a/b-binding protein	-9.07	0.001	-4.96	0.009	-7.02	0.000	AW397435	CAA45523	4.E-75
LHCII type III chlorophyll a/b binding protein	-9.06	0.001	-3.54	0.019	-1.62	0.004	AW472547	AAD27877	6.E-29
chlorophyll a/b-binding protein type III	-7.95	0.000	-3.36	0.037	-10.81	0.000	AI794678	S04125	2.E-43
chlorophyll a/b-binding protein CP24	-7.94	0.011	-3.40	0.002	-3.53	0.000	AW568252	AAD27882	8.E-72
chlorophyll a/b-binding protein CP24	-7.54	0.000	-5.72	0.003	-10.78	0.001	AI736217	AAD27882	3.E-41
chlorophyll a/b binding protein type II	-7.45	0.006	-3.69	0.048	-10.00	0.000	AI736285	AAL29886	3.E-18
LHCII type III chlorophyll a/b binding protein	-7.35	0.006	-3.23	0.007	-2.99	0.003	AW508739	AAD27877	2.E-22
photosystem I chlorophyll a/b-binding protein	-5.56	0.010	-2.38	0.015	-2.06	0.003	AW101657	CAA45523	1.E-75
chlorophyll a/b-binding protein CP24	-5.53	0.001	-5.23	0.012	-10.41	0.002	AW570380	AAD27882	6.E-88
chlorophyll a/b-binding protein type I	-5.39	0.000	-2.70	0.006	-3.23	0.004	AW100631	AAQ54512	1.E-36
photosystem I reaction center subunit III	-5.25	0.002	-4.83	0.030	-33.31	0.000	AW508794	AAD27880	1.E-82
chlorophyll a-b binding protein	-5.19	0.005	-4.23	0.016	-8.21	0.001	AW471940	P13869	2.E-85
photosystem II protein	-4.91	0.009	-2.91	0.003	-1.72	0.004	AW508451	AAM61462	6.E-07
oxygen-evolving enhancer protein 1	-4.74	0.005	-3.13	0.028	-5.54	0.000	AW472001	P14226	4.E-71
RuBisCO small subunit 1	-4.74	0.003	-5.01	0.107	-58.93	0.000	AW278725	CAA23736	7.E-53
photosystem I subunit X precursor	-4.65	0.014	-3.72	0.009	-4.81	0.000	AW277960	AAL32043	4.E-46
oxygen evolving enhancer protein 1	-3.99	0.014	-4.53	0.037	-14.93	0.000	AW568090	BAA96365	9.E-67
type II chlorophyll a/b binding protein	-3.61	0.000	-2.93	0.024	-9.04	0.001	AW100823	CAA57492	1.E-78
oxygen evolving enhancer protein 1	-3.42	0.011	-2.24	0.001	-1.70	0.001	AW101019	BAA96365	5.E-23
photosystem I psaH protein	-3.39	0.003	-2.98	0.002	-4.82	0.002	AW471851	AAQ21121	3.E-53
oxygen-evolving enhancer protein 1	-3.27	0.000	-1.82	0.009	-3.07	0.001	AI941034	P26320	3.E-39

Table S7 *(Continued from previous page.)*

	PEG mean	p-value	TUN mean	p-value	AZC mean	p-value	Clone accession #	Blast hit acession #	e-value
photosystem II reaction center W protein	-2.55	0.015	-1.74	0.024	-1.49	0.002	AW471847	CAA59409	1.E-28
oxygen-evolving enhancer protein 1	-2.11	0.030	-1.65	0.050	-1.58	0.005	AW567782	P26320	8.E-64
thylakoid membrane phosphoprotein	-1.93	0.004	-1.65	0.013	-2.03	0.011	AI960735	NP_566086	1.E-21
NADPH-protochlorophyllide oxidoreductase	-1.76	0.023	-2.08	0.009	-2.16	0.015	AW277941	BAA21089	4.E-78
Class: hormone metabolism									
1-aminocyclopropane-1-carboxylate oxidase	-6.79	0.010	-5.34	0.020	-11.62	0.000	AW508290	AAX84675	3.E-86
putative auxin-amidohydrolase precursor	-4.23	0.001	-3.33	0.007	-8.72	0.000	AW278733	CAG32961	1.E-18
geranylgeranyl hydrogenase	-2.18	0.014	-1.89	0.003	-2.37	0.010	AW185978	AAD28640	9.E-48
cytochrome P450 monooxygenase	-1.86	0.009	-3.74	0.017	-2.98	0.027	AW507877	AAD38930	8.E-55
Class: others									
unknown	-10.74	0.006	-2.49	0.047	-1.79	0.001	AW568035		
granule-bound starch synthase Ib precursor	-7.20	0.008	-6.51	0.000	-17.58	0.000	AW472193	BAC76613	4.E-65
unknown	-6.56	0.002	-2.69	0.002	-3.33	0.000	AW568660		
ultraviolet-B-repressible protein	-5.24	0.003	-4.16	0.011	-10.16	0.000	AW317705	AAS58469	1.E-29
pepsin A	-5.01	0.024	-2.34	0.003	-4.01	0.004	AW568189	NP_196320	4.E-54
granule-bound starch synthase Ib precursor	-4.85	0.005	-5.28	0.001	-8.47	0.000	AW472190	BAC76613	8.E-78
selenium binding protein	-4.82	0.008	-4.94	0.021	-28.20	0.000	AW101647	CAC67501	6.E-50
unknown	-4.73	0.001	-4.19	0.043	-19.62	0.000	AW508120		
myo inositol 1-phosphate synthase	-4.42	0.000	-4.48	0.003	-5.52	0.001	AW100674	CAJ15162	5.E-56
ATP synthase gamma chain	-4.15	0.002	-2.71	0.010	-5.77	0.000	AW186038	CAA45150	5.E-80
ATP-dependent helicase	-3.97	0.003	-5.72	0.016	-12.70	0.000	AW570395	NP_850847	1.E-58
acid phosphatase	-3.69	0.000	-2.61	0.016	-4.07	0.001	AI930921	CAA11075	8.E-20
UDP-glucose 4-epimerase	-3.52	0.001	-2.64	0.001	-3.32	0.007	AI856802	Q43070	4.E-83
unknown	-3.28	0.008	-2.41	0.031	-1.67	0.020	AW508445		
unknown	-3.17	0.002	-2.02	0.008	-1.47	0.038	AW569116		
cinnamoyl-CoA reductase	-3.11	0.007	-4.27	0.004	-5.60	0.000	AW508388	AAY86360	5.E-60
phosphoglycerate kinase	-3.08	0.012	-2.44	0.009	-6.98	0.000	AW568791	AAF85975	2.E-18
transformer-SR ribonucleoprotein	-3.07	0.011	-2.82	0.000	-7.39	0.000	AW568037	CAA70700	3.E-38

Table S7 *(Continued from previous page.)*

	PEG mean	p-value	TUN mean	p-value	AZC mean	p-value	Clone accession #	Blast hit acession #	e-value
unknown	-3.07	0.008	-3.62	0.006	-3.41	0.033	AW101065		
unknown	-3.02	0.014	-2.91	0.005	-6.71	0.000	AW507853		
ATP synthase B' chain	-2.94	0.008	-3.25	0.013	-7.91	0.001	AW471917	CAA50520	4.E-24
putative cinnamoyl-CoA reductase	-2.91	0.004	-3.01	0.005	-1.68	0.010	AW101559	AAT39306	2.E-16
palmitoyl-acyl carrier protein thioesterase	-2.58	0.039	-1.71	0.021	-5.28	0.001	AW568268	AAD01982	3.E-25
ACT domain-containing protein	-2.57	0.032	-1.75	0.002	-1.58	0.043	AW508692	NP_565908	5.E-35
plastid ribosomal protein CS17	-2.47	0.008	-2.16	0.005	-4.58	0.000	AW508645	CAA77502	4.E-32
unknown	-2.40	0.007	-2.00	0.001	-1.65	0.016	AW100867		
aldose 1-epimerase-like protein	-2.36	0.009	-2.74	0.012	-2.26	0.000	AW507799	NP_566594	3.E-66
myo-inositol-1-phosphate synthase	-2.30	0.001	-1.71	0.011	-2.30	0.006	AI941146	AAK72098	7.E-95
glutamine synthetase precursor	-2.28	0.010	-2.17	0.007	-2.19	0.010	AI736144	AAK43833	4.E-66
chitinase-like protein	-2.20	0.015	-2.45	0.007	-2.81	0.001	AW508700	BAC81645	1.E-38
carboxylic ester hydrolase	-2.16	0.038	-3.73	0.023	-2.30	0.010	AW278929	NP_177281	2.E-51
unknown	-2.16	0.005	-1.58	0.009	-2.58	0.013	AW598111		
putative leukotriene-A4 hydrolase	-2.08	0.025	-1.67	0.019	-1.88	0.004	AW277270	AAM91766	3.E-50
unknown	-2.03	0.004	-1.97	0.001	-2.81	0.001	AW570244		
unknown	-2.03	0.025	-2.13	0.003	-3.51	0.000	AW471578		
unknown	-2.02	0.037	-3.36	0.009	-2.07	0.008	AW471729		
unknown	-1.85	0.003	-2.17	0.013	-2.01	0.000	AI941196		
plasma membrane polypeptide	-1.83	0.028	-2.05	0.005	-1.67	0.016	AW459777	CAB61742	1.E-40
unknown	-1.80	0.017	-2.27	0.015	-1.61	0.033	AW508640		
microsomal omega-3 fatty acid desaturase	-1.70	0.009	-1.71	0.012	-3.54	0.000	AI960953	BAC87757	1.E-86
granule-bound starch synthase Ib precursor	-1.67	0.004	-2.21	0.031	-2.16	0.006	AW508018	BAC76613	5.E-49
unknown	-1.64	0.006	-2.00	0.007	-3.58	0.001	AW164582		

Livros Grátis

(http://www.livrosgratis.com.br)

Milhares de Livros para Download:

Baixar livros de Literatura
Baixar livros de Literatura de Cordel
Baixar livros de Literatura Infantil
Baixar livros de Matemática
Baixar livros de Medicina
Baixar livros de Medicina Veterinária
Baixar livros de Meio Ambiente
Baixar livros de Meteorologia
Baixar Monografias e TCC
Baixar livros Multidisciplinar
Baixar livros de Música
Baixar livros de Psicologia
Baixar livros de Química
Baixar livros de Saúde Coletiva
Baixar livros de Serviço Social
Baixar livros de Sociologia
Baixar livros de Teologia
Baixar livros de Trabalho
Baixar livros de Turismo